Revision 2

K-Bentonites: A Review

Warren D. Huff

Department of Geology, University of Cincinnati, Cincinnati, OH 45221 USA

Email: warren.huff@uc.edu

Keywords: K-bentonite, bentonite, tephra, explosive volcanism, volcanic ash

Abstract

Pyroclastic material in the form of altered volcanic ash or tephra has been reported and described from one or more stratigraphic units from the Proterozoic to the Tertiary. This altered tephra, variously called bentonite or K-bentonite or tonstein depending on the degree of alteration and chemical composition, is often linked to large explosive volcanic eruptions that have occurred repeatedly in the past. K-bentonite and bentonite layers are the key components of a larger group of altered tephras that are useful for stratigraphic correlation and for interpreting the geodynamic evolution of our planet. Bentonites generally form by diagenetic or hydrothermal alteration under the influence of fluids with high Mg content and that leach alkali elements. Smectite composition is partly controlled by parent rock chemistry. Studies have shown that K-bentonites often display variations in layer charge and mixed-layer clay ratios and that these correlate with physical properties and diagenetic history. The following is a review of known K-bentonite and related occurrences of altered tephra throughout the time scale from Precambrian to Cenozoic.

Introduction

Volcanic eruptions are often, although by no means always, associated with a profuse output of fine pyroclastic material, tephra. Tephra is a term used to describe all of the solid material produced from a volcano during an eruption (Thorarinsson, 1944). Tephra is well known to travel great distances – even across continents – and can thus serve to link not only volcanic zones but also to bind stratigraphic provinces together internally, and with each other. While residence time in the atmosphere of the very finest of these particles can be substantial, the deposition of the bulk of volcanic ejecta can be considered instantaneous on geological timescales. Often these volcanic products can be identified by various chemical and non-chemical means and if the eruption date is known, the occurrence of tephra from a given eruption in stratigraphic sequences provides a powerful means of dating such deposits, or of refining available dating schemes. Furthermore, the occurrence of tephra from the same eruption preserved simultaneously in various types of depositional environments including glacial, terrestrial and marine holds the potential of linking the regional causes of tectonic and stratigraphic change. In practice, tephrochronology requires tephra deposits to be characterized (or fingerprinted) using physical properties evident in the field together with those obtained from laboratory analyses. Such analyses include mineralogical and petrographic examination or geochemical analysis of glass shards or phenocrysts using an electron microprobe or other analytical tools including laser-ablation-based mass spectrometry or the ion microprobe. Tephrochronology provides the greatest utility when a numerical age obtained for a tephra is transferrable from one site to another using stratigraphy and by comparing and matching, with a high degree of likelihood, inherent compositional features of the deposits. Used this way, tephrochronology is an age-equivalent dating method that provides an exceptionally precise volcanic-event stratigraphy.

Bentonite is a clay deposit most commonly generated from the alteration of volcanic tephra, consisting predominantly of smectite minerals, usually montmorillonite. Other smectite group minerals may include hectorite, saponite, beidellite and nontronite. Bentonite was originally known as ‘mineral soap’ or ‘soap clay.’ As has been reported by numerous authors (e.g. Grim & Güven 1978), Wilbur C. Knight first used the name taylorite for this material in an article in the Engineering and Mining Journal (1897). The name came from William Taylor of Rock River, Wyoming; owner of the Taylor ranch where the first mine was located. Taylor made the first commercial shipments of the clay in 1888. After Knight learned that the name taylorite had been previously used in England for another mineral he decided to rename the clay bentonite (Knight 1898) in recognition of its occurrence in the Cretaceous Fort Benton Group of the Mowry Formation. The Fort Benton Group was named after Fort Benton, Montana in the mid-19th century by F.B. Meek and F.V. Hayden of the U.S. Geological Survey (1862, this report described the rocks of Nebraska, which at that time included Wyoming, Montana and Dakota). As later defined by Ross and Shannon (1926), "Bentonite is a rock composed essentially of a crystalline clay-like mineral formed by the devitrification and the accompanying chemical alteration of a glassy igneous material, usually a tuff or volcanic ash." Bentonite deposits are considered instantaneous at geologic scales, because of the briefness of volcanic explosions and the short duration over which particles are transported in the troposphere/stratosphere and finally deposited in sedimentary basins. Resulting from paroxysmal volcanic explosions (Plinian or ultra-Plinian events, co-ignimbrite), ash is deposited on surfaces of several hundreds to thousands of km^2, thus allowing intrabasinal or interbasinal long-range correlations, which can be compared with biostratigraphic units. Bentonites should also provide precise radiometric ages by isotopic analysis (Ar/Ar, U/Pb) of primary crystals from the magma (e.g., zircon, biotite, feldspar). Geochemical characterization, including immobile elements (Ta, Th, U, Nb, Hf, etc.) and Rare Earth Elements (REE), provide information on Jurassic paleovolcanism and active volcanic sources.

One of the earliest detailed descriptions of K-bentonites was provided by Hagemann and Spjeldnæs (1955), who reported on a Middle Ordovician section in the Oslo-Asker district of Norway that contained twenty-four bentonite beds ranging in thickness from 130 cm to less than 0.5 cm. The authors acknowledged that they were called bentonites because they appear as thin, light layers, which expand when placed in water. But they go on to point out that as the bentonites have been metamorphosed by slippage along the bedding planes during later tectonic movements, the clay cannot any longer be considered as "real" bentonite. Ross (1928) suggested the name metabentonite for such altered bentonites. In the Sinsen bentonites, however, Hagemann and Spjeldnæs (1955) concluded that all the material had been altered, and it would therefore be better to use another name. Weaver (1953) used the name potassium-bentonites (K-bentonites) for bentonites rich in potassium, in order to distinguish them from other bentonites, and thus this designation became embedded in the literature. In stratigraphy and tephrochronology, completely or partially devitrified volcanic ash fall beds may be referred to as K-bentonites since over time, burial diagenesis begins to convert smectite to mixed-layer illite/smectite (I/S) through the addition of non-exchangeable potassium in the interlayer position. Under certain circumstances altered ash fall layers typically associated with coal may become kaolinite-dominated and are commonly referred to as tonsteins.

The purpose of this review is to examine a variety of K-bentonite and related tephrochronology applications ranging from Late Precambrian to Cretaceous. The volcanological background to tephrochronology as a method along with attendant techniques and regional applications have been summarized a number of times in recent years, such as the one by Lowe (2011), whose very comprehensive review covers a broad range of geological, archaeological and anthropological studies. The aim of the present review is therefore not to provide a comprehensive treatment of tephrochronology, but to focus on examples that highlight some of its strengths and limitations where K-bentonites and related altered tephras occur in specific geological settings.

Proterozoic K-bentonites

Recent studies, such as those by Bouyo Houketchang et al. (2015), Decker et al. (2015) and Karaoui et al. (2015) have added substantially to the body of knowledge regarding altered

Proterozoic tephras and their application to tephrochronology. Two studies involving K-bentonites are described in more detail.

Twenty silicified volcanic tephras ranging in age from 531.1 ±1 to 548.8 ±1 Ma (Grotzinger et al. 1995) have been identified in the Kuibis and Schwarzrand subgroups of the terminal Proterozoic Nama Group of Namibia (Saylor et al. 2005). Nineteen of the Nama ash beds are in the Schwarzrand Subgroup in the Witputs subbasin. Two of these are in the siliciclastic dominated lower part of the subgroup, which consists of the Nudaus Formation and Nasep Member of the Urusis Formation and comprises two depositional sequences. Identification and correlation of these ash beds are very well known based on stratigraphic position. Sixteen ash beds are contained within the carbonate-dominated strata of the Huns, Feldschuhhorn and Spitskop members of the Urusis Formation. These strata comprise four large-scale sequences and eighteen medium-scale sequences. Ash beds have been found in three of the large-scale sequences and seven of the medium-scale sequences. Correlations are proposed for these ash beds that extend over large changes in facies and stratal thickness and across transitions between the seaward margin, depocenter and landward margin of the Huns-Spitskop carbonate shelf (**Figure 1**). A study of whole rock and in situ phenocryst compositions was conducted to evaluate the feasibility of independently testing sequence stratigraphic correlations by geochemically identifying individual ash beds. Whole rock abundances of Al, Fe, Mg, K and Ti vary inversely with Si, reflecting variations in phenocryst concentration due to air fall and hydrodynamic sorting. These sorting processes did not substantially fractionate whole rock rare earth element abundances (REE), which vary more widely with Si. REE abundances are higher in samples of the Nudaus ash bed than in samples of the Nasep ash bed, independent of position in bed, phenocryst abundance, or grain size, providing a geochemical means for discriminating between the two beds. Variations in the position of chondrite-normalized whole rock REE plots similarly support suspected correlations of ash beds between widely separated sections of the Spitskop Member. Abundances of Fe, Mg and Mn in apatite plot in distinct clusters for Spitskop ash beds that are known to be different and in clusters that overlap for ash beds suspected of correlating between sections. Abundances of REE in monazites differ for the Nudaus, Nasep and Spitskop ash beds in which these phenocrysts were identified. Multivariate statistical analysis provided a quantitative analysis of the discriminating power of different elements and found that whole rock abundances of Ge, Nb, Cs, Ba and La discriminate among the whole rock compositions of the Nudaus and Nasep ash beds and the Spitskop ash beds that are thought to correlate between sections.

Su et al. (2008) reported Sensitive High Resolution Ion Microprobe (SHRIMP) U–Pb zircon ages from illite- and I/S-rich K-bentonite beds from different locations in the Xiamaling Formation near Beijing at the northern margin of the North China Craton. The 1379 ±12 Ma and 1380 ±36 Ma ages obtained in their study assign a Mid-Mesoproterozoic (Ectasian Period) age for the formation. In addition, they concluded that this succession northwest of Beijing can be correlated with that of the well-known Meso- to Neoproterozoic standard section in Jixian, east of Beijing.

Cambrian K-Bentonites

In a study of Lower Cambrian K-bentonites from the Yangtze Block in South China Zhou et al. (2014) have shown that the widespread K-bentonites occur in two important stratigraphic levels: the middle Zhujiaqing Formation and the basal Shiyantou Formation and their lateral equivalents (**Figure 2**). Biostratigraphically, the older K-bentonite bed is preserved in the *Anabarites trisulcatus* – *Protohertzina anabarica* assemblage zone and the younger K-bentonite in the poorly fossiliferous interzone. In outcrop, the K-bentonites have different colors (white, blackish gray, and yellow), which are distinct from their adjacent strata (phosphorites, black shales, cherts, and dolostones). The Lower Cambrian K-bentonites crop out in the shallow-water platform interior and in the deep-water transitional zone of the Yangtze Block. Representative Lower Cambrian K-bentonite sections in the platform interior include the Meishucun, Wangjiawan, Maidiping, Gezhongwu, Yankong, Songlin and Taishanmiao sections.

The Meishucun section is a former global stratotype candidate section for the Precambrian/Cambrian boundary. At this section, a K-bentonite locally up to 2.6 m and two ca. 10 cm K-bentonite beds occur in the middle Zhujiaqing Formation and the bottom of the Shiyantou Formation, respectively. The Wangjiawan section also lies in Jinning County and is about 23 km southeast of the Meishucun section. Lithostratigraphic units of this section are highly similar to those of the Meishucun section. In the Wangjiawan section a 20 cm K-bentonite and a 10 cm K-bentonite were discovered near the base of the Shiyantou Formation and the middle Zhujiaqing Formation at the Wangjiawan section, respectively. Due to the scarce fossil records, the biostratigraphical position of the K-bentonites in the deep-water realm of the Yangtze Block is still unclear. However, the K-bentonites are below a regionally widespread Ni-Mo polymetallic layer, which is under the horizon hosting the oldest trilobites in South China. Thus, Zhou et al. (2014) were able to confirm that the K-bentonites recognized in the deep-water region of the Yangtze Block are distributed in the pre-trilobite strata.

A previous study by Chen et al. (2009) shows that the top of the Liuchapo Formation preserves a K-bentonite (referred to as tuff by the authors) with a SHRIMP U-Pb age of 536 ±5.5 Ma, which is consistent with an earlier age of 538.2 ±1.5 Ma reported for a K-bentonite in the corresponding Zhongyicun Formation in northeast Yunnan Province (Jenkins et al. 2002).

Mineralogical studies on the Lower Cambrian K-bentonites in eastern Yunnan Province by Zhang et al. (1997) showed that the <2 μm clay fraction of the K-bentonites consists of illite, mixed-layer I/S, and kaolinite and that the non-clay-mineral composition of the coarse fraction consists of sanidine, pyrite, collophanite, glauconite, and beta-form quartz. In addition the clay fraction of the K-bentonite in the base of the Niutitang Formation at the Songlin section in Guizhou Province was analyzed using X-ray diffraction. In the air-dried sample prominent peaks at 10.6 Å, 5.0 Å and 3.33 Å indicate a predominantly illite phase but with a small amount of mixed-layer I/S. Saturation with ethylene glycol broadens the first-order reflection further to reveal two components at 11.0 Å and 9.8 Å. The second-order peak is shifted slightly to 5.10 Å indicating a ratio of 10% smectite and 90% illite (Moore and Reynolds 1997). Upon heating to 350^{o} C the expanded phase collapses to 10.0 Å. Peaks at 4.48 Å and 3.30 Å reflect the presence of a small amount of iron sulfate, and peaks at 3.33 Å overlapping the illite peak and at 4.24 Å belong to trace amounts of clay-size quartz. Meanwhile, primary volcanogenic phenocrysts such as euhedral quartz, euhedral to sub-euhedral prismatic zircon, and euhedral sanidine were discovered in the coarse fraction of the K-bentonites from various sections in this study.

Immobile trace elements have been used by numerous workers (Huff et al. 2000; Astini et al. 2007; Su et al. 2009) to provide information on the magmatic composition of K-bentonite ashes and on the tectonic setting of the source volcanoes. TiO_2 and the trace elements Zr, Nb, and Y are commonly considered to be immobile under processes of weathering, diagenesis, and low-grade metamorphism, and are thus useful indicators of past rock history. The Nb/Y ratio is widely used as an index of alkalinity and Zr/TiO_2 as a measure of differentiation. According to the Nb/Y and Zr/TiO_2 ratios of igneous rocks of known origin, Winchester and Floyd (1977) generated a plot of Nb/Y against Zr/TiO_2 that is organized around the petrology of the original rock type. The Lower Cambrian K-bentonite samples studied by Zhou et al. (2014) plot in the fields of trachyte, trachyandesite, rhyodacite, and rhyolite, suggesting that the K-bentonites are most probably derived from felsic magmas with subalkaline to alkaline composition. Compared with the K-bentonite in the basal Shiyantou Formation and its equivalent sequence, the K-bentonite in the middle Zhujiaqing Formation and its correlative succession is characterized by lower Zr and Nb concentrations.

The volcanic activities that produced the tephras of two K-bentonite beds occurred during an interval of tectonic transformation, and the source volcanoes of the K-bentonites were probably located in the east margin of the Ganze–Songpan Block. Furthermore, the correlation results of the two important Lower Cambrian K-bentonite beds indicate that the previous placement of the Precambrian/Cambrian boundary in South China at the polymetallic Ni-Mo layer in the lowermost Niutitang Formation is inappropriate. Zhou et al. (2013) reported a SHRIMP U-Pb geochronology study of the K-bentonite in the topmost Laobao Formation at the Pingyin section, Guizhou, South China. Their results yielded an age of 536 ±5 Ma, suggesting that the K-bentonite here can be correlated with the intensely studied K-bentonite within the middle Zhongyicun Member of the Zhujiaqing Formation at the Meishucun section in Yunnan. The age of the K-bentonite at the Pingyin section implies that the overlying polymetallic Ni-Mo layer should be younger than 536 ±5 Ma. Hence the previous placement of the Precambrian/Cambrian boundary at this layer is inappropriate. Combined with the results of stratigraphic correlations, Zhou et al. (2013) suggested that the K-bentonites in the middle Zhongyicun Member of the Zhujiaqing Formation and the base of the Shiyantou Formation, together with the polymetallic Ni-Mo layer, serve as three important marker beds. Their self-consistent radiometric ages are considered to have established an improved geochronologic framework for the Lower Cambrian in South China. Combined with published geochronological data, Zhou et al. (2014) concluded that the boundary should be placed within the strata beneath the K-bentonite in the middle Zhujiaqing Formation and its correlative stratigraphic level (**Figure 3**).

Ordovician K-bentonites

As with every Phanerozoic System, many Ordovician successions contain a number of K-bentonites representing episodes of explosive volcanism, most commonly associated with collisional tectonic events (Huff et al. 2010). Perhaps the earliest report of an Ordovician bentonite was a study by Allen (1929) who reported finding near the base of the Decorah shale in Minnesota a thin clay layer consisting of montmorillonite and retaining what he described as a pumiceous texture and containing sanidine, quartz, biotite, apatite, and zircon representing an altered pyroclastic deposit. His work cited previous studies, such as the one by Ross and Shannon (1926). **Figure 4** shows the global stratigraphic and geographic distribution of K-bentonite beds that have been reported in the literature. Numerous beds have been reported from North and South America, Asia and Europe. A brief review will summarize some of the pertinent literature for each region.

North America

The Ordovician successions of North America are known to contain nearly 100 K-bentonite beds, one or more of which are distributed over 1.5 x 10^6 km^2 (Kolata et al. 1996). The first report of an Ordovician K-bentonite in North America was made by Ulrich (1888) who described a thick bed of clay in the upper part of what is now known as the Tyrone Limestone, near High Bridge, Kentucky. The Tyrone Limestone, along with the Camp Nelson Limestone and the Oregon Formation constitute the High Bridge Group of Late Ordovician age. Subsequent work by Nelson (1921, 1922) showed that the bed was volcanogenic in origin and that it could be correlated into Tennessee and Alabama. From the 1930's on, K-bentonite beds of Ordovician age began to be reported from localities throughout eastern North America (Brun and Chagnon 1979; Huff and Kolata 1990; Kay 1935; Kolata et al. 1996; Weaver 1953). Their clay mineralogy is typically dominated by a regularly interstratified I/S in which the montmorillonite swelling component accounts for 20-40 percent of the total structure. Two prominent K-bentonites occur within the Tyrone Limestone of central Kentucky (**Figure 4**). The Millbrig or "Mud Cave" K-bentonite of local drillers is found at or near the contact between the Tyrone Limestone and the overlying Curdsville Limestone Member of the Lexington Limestone. In parts of the region it has been removed along the pre-Lexington disconformity (Cressman 1973) and hence has somewhat restricted usefulness in regional correlation. The equivalent bed in the Carters Limestone of central Tennessee is the T-4 bed of Wilson (1949). The Deicke or "Pencil Cave" K-bentonite of local usage occurs approximately 4 to 6 m below the top of the Tyrone Limestone and varies in thickness from a few centimeters to 1.5 m (**Figure 5**). Some reworking of the original ash by waves and bottom currents undoubtedly occurred. However, the influx of terrestrial clastics was so minimal as to preclude contamination of the K-bentonite by anything other than carbonate mud. The Deicke is the most persistent K-bentonite marker in the area. Its equivalent in central Tennessee is the T-3 bed (Wilson 1949). The chemical characteristics of the K-bentonite beds along the Cincinnati arch were reported by Huff and Türkmenoglu (1981).

Using immobile trace elements the Deicke and Millbrig have been correlated by chemical fingerprinting from southeastern Minnesota to southeastern Missouri (Kolata et al. 1987) and by wireline logs from Missouri to the southern Appalachians and into the Michigan Basin and southern Ontario (Huff and Kolata 1990; Kolata et al. 1996). Both beds range from 1.5 m or more in thickness in the southern Appalachians (Haynes 1994) to 3 cm or less in western Iowa. Unpublished data from wireline logs and recent studies (Leslie et al. 2006) of the Bromide Formation in southern Oklahoma suggest that both beds extend farther to the southwest than has previously been mapped. Other K-bentonites include a thin (5-6 cm) widespread but locally absent bed about 24 m below the top of the Tyrone Limestone, another thin bed between the Deicke and Millbrig, and a bed in the Curdsville Member of the Lexington Limestone which Conkin and Conkin (1992) labeled the Capitol Metabentonite. Huff et al. (1996a) calculated the dense rock equivalent (DRE) values to be 943 km^3 for the Deicke and 1509 km^3 for the Millbrig.

Kolata et al. (1996) documented the stratigraphic distribution of at least seven named K-bentonites beds traceable throughout the mid-Mohawkian of the upper Mississippi Valley region, and subsequently named them the Hagan K-bentonite complex (Kolata et al. 1998). The Deicke and

Millbrig beds are part of the complex and, to date, have the widest known distribution. A unique feature of the Hagan complex is that it straddles the Black River-Trenton unconformity, generally believed to be a significant stratigraphic sequence boundary in the eastern United States (Holland and Patzkowsky 1996) and is itself traceable throughout much of the southern and central Appalachians. Bergström et al. (2010) produced a transatlantic correlation diagram (**Figure 6**), showing the relations between conodont, graptolite, and chitinozoan biostratigraphy, K-bentonite event stratigraphy, and the early Chatfieldian $\delta^{13}C$ excursion in North America and Baltoscandia. On the basis of these relations, the GICE (Guttenberg isotope carbon excursion) is considered the same $\delta^{13}C$ excursion as the "middle Caradocian" excursion of Kaljo et al. (2004).

South America

Ordovician K-bentonites have been recognized since 1994 in the upper San Juan Limestone and overlying clastic strata of the Gualcamayo and Los Azules formations in the Argentine Precordillera (Huff et al. 1998; Bergström et al. 1996). The widespread occurrence of K-bentonite beds in the Argentine Precordillera constitutes one of the most extensive suites of such beds known anywhere in the Ordovician System of the world and serves as testimony to the high intensity of explosive volcanism along this margin of Gondwana during the early and middle parts of that period. Previous and ongoing studies of the sedimentology, mineralogy, and geochemistry of these beds provide both insight and constraints concerning the magmatic, tectonic, and paleogeographical settings under which the explosive volcanism was generated, and also permit comparisons with lower Paleozoic K-bentonites on other continents. While the most recent field work has revealed an extensive succession of K-bentonite beds in the exposures along the Gualcamayo River and its tributaries in western La Rioja Province, detailed particle-size, mineralogical, and geochemical studies on samples from the extensive sections at Cerro Viejo, near Jáchal, and at Talacasto, north of San Juan, in San Juan Province show typical collision margin tectonovolcanic settings (Huff et al. 1998) (**Figures 7-8**). Furthermore, while most known evidence for pre-Andean explosive volcanism on the Gondwana margin is preserved in the Ordovician sections of the Argentine Precordillera, additional beds of pyroclastic origin have also been reported from the Balcarce Formation of the Tandilia region, south of Buenos Aires (Dristas and Frisicale 1987). Trace fossils have traditionally been used to assign the Balcarce Formation to the Lower Ordovician, due to the presence of *Cruziana furcifera* (Poiré et al. 2003). At least one, and perhaps as many as four, altered pyroclastic beds occur in the white quartzite sequence which ranges from 18 to 500 m in thickness and unconformably overlies Precambrian basement (Dalla Salda et al. 1988). In contrast to the I/S-rich beds of the Precordillera, the Balcarce beds consist mainly of well crystallized kaolinite with occasional crystals of altered ilmenite, and are considered to be tonsteins that are the product of altered mafic ashes (Dristas and Frisicale 1987).

The Argentine sequence is nearly unique in both the number and lateral distribution of K-bentonite beds, and geochemical and grain-size data are consistent with a source area along the Gondwana margin, such as the Puna-Famatina arc (Huff et al. 1998). They provide no supporting evidence of a close association between the Precordillera and Laurentian sedimentary basins at that time, as has been proposed by Thomas and Astini (1996).

Northern and Central Europe

The closing of the Iapetus Ocean separating Baltica, Avalonia, and Laurentia occurred by means of the subduction of oceanic crust beneath, and the consequent collision of, volcanically active island arcs or microplates against the southeastern margin of Laurentia (Scotese and McKerrow 1991). An Early to Mid Ordovician (ca. 465-480 Ma) magmatic and tectonometamorphic event is well documented in the Karmøy-Bergen area (southern Norway) and in the Helgeland Nappe Complex (Uppermost Allochthon, north-central Norway) (Nordgulen et al., 2003).

In the Late Ordovician to Early Silurian (ca. 450-430 Ma) gabbroic to granitic plutons were emplaced into the earlier assembled oceanic and continental rock units. The plutons show evidence of mixed crust and mantle sources and probably represent continued magmatism along the Laurentian margin. These collisions were associated with the Taconic orogeny, which began during the Mid Ordovician and produced a complex deformational and sedimentological record that has been extensively documented (Rowley and Kidd 1981; Stanley and Ratcliffe 1985; Tucker and Robinson 1990) and which includes numerous K-bentonite beds in both the eastern North American, British, and Baltoscandian successions. Baltica was surrounded by a passive margin during the Middle Ordovician, but it apparently was in close proximity to Laurentia (Cocks and Torsvik 2005; Huff et al. 1992; McKerrow et al. 1991). Consequently, the origin of the approximately 150 Middle-Upper Ordovician ash beds in southern Sweden, including the Kinnekulle K-bentonite, can be attributed to the explosive volcanic activity in the magmatic arcs associated with the Taconian Orogeny. Bergström et al. (1995) subdivided the twenty-four tephra layers described by Hagemann and Spjeldnæs (1955) into four separate complexes that could be correlated to bentonites in Sweden and Estonia: the 1) Grefsen K-bentonite complex (nineteen lowest layers); 2) the Sinsen K-bentonites (two layers); 3) Kinnekulle K-bentonite (the thickest layer) and the 4) Grimstorp K-bentonites (uppermost two layers). Note that K-bentonites in other regions of Baltica are also identified at higher stratigraphic levels than in Oslo, well into the Katian (Huff 2008). In addition to the Sinsen locality, Bergström et al. (1995) identified the Kinnekulle and Grimstorp layers in a road section in Vollen, Norway near the type locality for the Arnestad Formation.

Figure 9 shows the comparative stratigraphic distribution of Ordovician K-bentonites in Baltoscandia and in North and South America. Many beds are coeval, most notably the Viruan Kinnekulle bed in Baltoscandia and the Mohawkian Millbrig bed in North America. The possibility of a common source for the Millbrig and Kinnekulle giant ash beds was suggested by Huff et al. (1992), but subsequently questioned by Haynes et al. (1995). Close examination in the field shows that both beds consist of several internally graded units, suggesting that each bed represents the cumulative deposition of multiple ash falls in environments characterized by low background sedimentation rates. This aspect was examined in some detail by Kolata et al. (1998) and Haynes (1994) for the Millbrig and by Huff et al. (1999) for the Kinnekulle, all of whom showed systematic mineralogical and grain size variation within individual subunits. Given higher rates of sediment accumulation it is conceivable that these units could be preserved as a series of closely spaced coeval beds (Bergström et al. 1997b; Huff et al. 1999). Sell et al. (2013) found that the Millbrig K-bentonite from Kentucky and the Kinnekulle K-bentonite from Bornholm, Denmark yielded chemical abrasion thermal ionization mass spectrometry U–Pb zircon dates of 452.86 ±0.29 and 454.41 ±0.17 Ma, respectively. The stratigraphic position of these beds in England and Wales is essentially occupied by the massive Snowdon and Borrowdale volcanics of north Wales and the English Lake District, as described above, although a possible occurrence of the Kinnekulle K-bentonite in central Wales was reported by Bergström et al. (1995).

The Middle Ordovician section at Röstånga in Scania (southern Sweden) contains eighteen K-bentonite beds ranging from 1-67 cm in thickness, and all occur within the *D. foliaceus* (formerly *multidens*) graptolite biozone. At Kinnekulle, 290 km to the north, this interval includes the type section of the Kinnekulle K-bentonite, which is very widespread and has been correlated throughout northern Europe (Bergström et al. 1995). In most sections the Kinnekulle K-bentonite can be recognized by distinctive geochemical fingerprints, its prominent thickness, and by its biostratigraphic and lithostratigraphic position (Bergström et al. 1995). However, at Röstånga, whole rock chemistry is inconclusive at identifying which of the eighteen beds is the Kinnekulle K-bentonite. Several beds at Röstånga correlate equally well with the Kinnekulle bed (Bergström et al. 1997b) and thus argue strongly for the composite nature of what is called the Kinnekulle K-bentonite. The Deicke, on the other hand, appears to be a single event deposit but it has not been recognized in Europe.

Kiipli et al. (2014a) analyzed the content of Ti, Nb, Zr and Th in 34 Upper Ordovician bentonites from the Billegrav-2 drill core, Bornholm, Denmark. The section contains two 80-90 cm thick K-bentonites, which potentially may represent the Kinnekulle K-bentonite, as well as several rather thick but composite bentonite layers with thin terrigenous shale interbeds. Comparison of the four immobile trace elements with data from the Kinnekulle K-bentonite reported from other locations in Baltoscandia indicate that the 80 cm thick K-bentonite between 88.30 and 89.10 m in the Billegrav-2 core represents this marker bed. The other thick (90 cm) K-bentonite in the Billegrav-2 core, exceeding the thickness of the Kinnekulle K-bentonite, belongs to the Sinsen or uppermost Grefsen Series K-bentonites.

The regional aspects of ash accumulation on submarine surfaces has been discussed by Kolata et al. (1998) and Ver Straeten (2004). The Millbrig in eastern North America and the Kinnekulle in northern Europe both display macroscopic and microscopic evidence of multiple event histories, a characteristic that is only explainable by invoking a history of closely spaced episodic ash accumulations in areas with essentially no background sedimentation (Kolata et al. 1998; Ver Straeten 2004). Portions of the Millbrig and Kinnekulle beds have biotite grains that are compositionally indistinguishable from one another, although the majority of samples analyzed show a clear distinction between the two beds based on Fe, Mg and Ti ratios. Tectonomagmatic discrimination diagrams combined with Mg number data indicate that the Deicke-Millbrig-Kinnekulle sequence represents the transformation from calc-alkaline to peraluminous magmatic sources, consistent with a model of progressively evolving magmatism during the closure of the Iapetus Ocean (Huff et al. 2004). Published isotopic age dates are inconclusive as to the precise ages of each bed. Thus, it appears that the Millbrig and Kinnekulle beds are coeval and represent separate but simultaneous episodes of explosive volcanism, although it cannot be excluded that parts of these beds were derived from the same eruption(s). Similar intercontinental correlations elsewhere in Europe or China have not yet been attempted.

While most Ordovician K-bentonites reported in Europe are from the British Isles (Fortey et al. 1996; Huff et al. 1993; Millward and Stone 2012) and Baltoscandia (Bergström et al. 1995; Bergström et al. 1997b), there are also occurrences in Poland (Tomczyk 1970), the Carnic Alps (Histon et al. 2007) and Lithuania (Sliaupa 2000). The Alpine orogen represents a collage of Alpine and Prealpine crustal fragments. Schönlaub (1992, 1993) has shown that some fragments reflect a true odyssey of near global wandering. These segments have been dated as ranging from Late Ordovician to Permian based on various rather well-known climate sensitive biofacies and lithofacies markers, thus adding further to the controversy with regard to the paleogeography and the relationship of the Paleozoic proto-Alps and the coeval neighboring areas such as Baltica, the British Isles, the Prague Basin (Barrandian), Sardinia, Southern France and Spain and North Africa. Ninety-five K-bentonite levels have been recorded to date from the Upper Ordovician (Ashgill) to Lower Devonian (Lochkov) sequences of the Carnic Alps (Histon et al. 2007) (**Figure 10**). They occur in shallow to deep-water fossiliferous marine sediments, which suggests a constant movement from a moderately cold climate of approximately 50° southern latitude in the Upper Ordovician to the Devonian reef belt of some 30° south.

Recently, Huff et al. (2014) reported the discovery of eight K-bentonite beds in the Late Ordovician of the Tungus basin on the Siberian Platform. All the beds were identified in the outcrops of the Baksian, Dolborian and Burian regional stages, which correspond roughly to the Upper Sandbian, Katian and probably lowermost Hirnantian Global Stages. The three lowermost beds from the Baksian Regional Stage were studied in detail and are represented by thin beds (1.2

cm) of soapy light-gray or yellowish plastic clays. They can be traced in the outcrop over a distance of more than 60 km along the Podkamennaya Tunguska River valley. Zircon crystals from the uppermost K-bentonite bed within the Baksian Regional Stage provide a $^{206}Pb/^{238}U$ age of 450.58 ±0.27 Ma. This appears to be nearly the same age as the Haldane and Manheim beds in North America. The Manheim is in the *Diplacanthograptus spiniferus* graptolite Zone and the Haldane is likely within the upper part of the *Belodina confluens* conodont Zone, which indicates the bed would be mid-Katian and latest Mohawkian. The timing of volcanism is surprisingly close to the period of volcanic activity of the Taconic arc near the eastern margin of Laurentia. Thus, it appears that the Taconic arc has its continuation along the western continental margin of Siberia so that they constitute a single Taconic-Yenisei volcanic arc.

China

The first Ordovician K-bentonite recognized in China (Ross and Naeser, 1984) was a single bed in the Upper Ordovician Wufeng Shale. Subsequently, Huff and Bergström (1995) reported two beds in the Lower Ordovician Ningkuo Formation at Hentang in the Jiangshan Province, southeastern China. More recently, a number of K-bentonite beds have been recognized in the Ordovician-Silurian transition (Ashgill - early Llandovery) in the Yangtze Block, south China (Su et al. 2004). A preliminary analysis of the geochemical composition of the K-bentonites has suggested a parental magma origin of trachyandesite to rhyodacite with some rhyolite, which came from volcanic-arc and syn-collision to intra-plate tectonic settings. Regional correlation of these K-bentonite beds indicates that they clearly have the potential of increasing southeastward both in thickness and grain-size. These features suggest that the original volcanic ash may come from the southeastern part of the present-day south China.

In addition, along the southeast margin of the Yangtze Block, typical flysch successions have also been identified both from the Zhoujiaxi Group (early Llandovery) and Tianmashan

Formation (Ashgillian) in the southern part of Hunan Province, south China. Geochemical analysis on the silicate minerals has suggested that the flysch successions were deposited in the basin on a passive continental margin (Fletcher et al. 2004). Field observations on the paleo-currents, cross-beddings, ripple marks as well as flute marks, all suggest that the detrital components must have been transferred from the southeast part of the present south China, in good agreement with the conclusion drawn from the analysis of the K-bentonites as mentioned above. Furthermore, the flysch successions both in the Tianmashan Formation and Zhoujiaxi Group clearly show a northwestward progradation in space and time during the Ordovician-Silurian transition. Both the K-bentonites and flysch successions could be regarded as the products of collision volcanism in the area to the continuous northwestward collision and accretion process of the Cathaysia and Yangtze Blocks (Su et al. 2009) (**Figure 11**).

Silurian K-bentonites

Baltoscandia and the British Isles

Silurian K-bentonite beds occur throughout northern Europe. Some of the beds occur only at local scales while others appear to be widespread on a regional scale. More than 100 K-bentonite beds occurring in Llandovery through Ludlow strata of the Welsh Borderlands were described by Huff et al. (1996b) (**Figure 12)**. K-bentonite sequences are preserved in the deep water Llandovery Purple Shales, the off-lap facies of the Wenlock Series, turbiditic facies of the Welsh Basin, slope facies of the early Ludlow Eltonian Beds and carbonate platform deposits of mid-Ludlow to late-Ludlow Bringewoodian Beds. Individual beds range from 2 cm to l m in thickness and typically consist of white to greenish-grey plastic clay with minor amounts of mainly volcanogenic, non-clay minerals. The <2 μm fractions of the K-bentonites consist of random to regularly interstratified (RO to R3) I/S with lesser amounts of discrete illite, chlorite and kaolinite. Non-clay minerals include a volcanic suite of quartz, biotite, apatite, zircon, sanidine and albite-oligoclase. K-Ar ages of illite in the I/S are positively correlated with the percent of illite, indicating evidence of a slow and continuous process of illitization from the Silurian to the end of the Paleozoic.

Kiipli et al. (2010) described the distribution of K-bentonites and Telychian chitinozoans in four East Baltic drill core sections in Latvia and Estonia and combined it with graptolite and conodont biozone data to give a precise correlation chart. Thickness variations in the K-bentonites suggest that the source of the volcanic ash was to the west and northwest. A detailed study of two Lithuanian drill core sections by Kiipli et al. (2014b) extended previous knowledge of the occurrence and composition of K-bentonites to the south. In the Lithuanian sections one K-bentonite was found in the Rhuddanian, five K-bentonites were recognized in the Aeronian, 17 K-bentonites in the Telychian, 26 in the Sheinwoodian, 10 in the Homerian and six in the Ludlow. All K-bentonites found in Lithuania are characterized by the main component of sanidine. The identification of graptolite species allowed K-bentonites to be assigned their proper stratigraphic positions. Silurian K-bentonites in Lithuania are generally characterized by broad X-ray diffraction reflections of the main component of sanidine phenocrysts, suggesting poor crystallinity. Only fourteen of the 69 samples studied contained sanidine with a sharp reflection, which gave the best correlation potential. A large number of Lithuanian K-bentonites are not known in Latvia and Estonia, indicating that volcanic ashes reached the East Baltic area from two source regions, the Central European and Norwegian Caledonides.

The designation of the Osmundsberg K-bentonite, named after a carbonate mound known as Osmundsberget in the Siljan area in Dalarna, Sweden, was proposed for one of the thickest and most widespread beds (Bergström et al. 1998b), and this bed has been traced from Estonia across Sweden to the British Isles using primarily biostratigraphic criteria. However, the occurrence of numerous K-bentonite beds in the investigated regions coupled with a lack of continuity of some individual beds, and a lack of consistently good biostratigraphic control, created some difficulties in correlating the Osmundsberg K-bentonite bed over long distances (**Figure 13**).

In order to provide a high-resolution chemostratigraphic correlation of the Osmundsberg K-bentonite, and to test the stratigraphic usefulness of fingerprinting in regional correlations of Silurian K-bentonites in Baltoscandia, Inanli et al. (2009) plotted chemical data on a series of binary diagrams using several of the most effective discriminating elements and elemental ratios, and discriminant function analysis was performed using data for 20 trace elements in 16 samples of the Osmundsberg K-bentonite and 24 other Silurian K-bentonite beds. The Osmundsberg K-bentonite beds were biostratigraphically grouped and discriminant analysis was used to test the hypothesis that such groups also have unique chemical characteristics. The use of discriminant analysis in these models supported the correlation of the Osmundsberg K-bentonite bed in Baltoscandia as proposed by Bergström et al. (1998b). However, five K-bentonite samples, originating from Sweden, Denmark, Scotland, Wales and Northern Ireland that were initially considered to be correlative with the Osmundsberg were found to have trace element compositions that separate them statistically from the Osmundsberg. Apart from these five samples, the models were able to separate 100% of the group members as identified by their biostratigraphic position. Once the criteria for membership was established by the discriminant functions a test of the two suspected Osmundsberg equivalents from Scotland was carried out. One of these samples, DL 3, from Dob's Linn, Scotland (**Figure 14**), was correlated with the Osmundsberg with a high degree of confidence on the basis of its chemical composition.

Ukraine

The Dnestr Basin of Podolia, in southern Ukraine, contains one of the best-known and most complete Middle-Upper Silurian sections in northern Europe, and one of the most intensively studied Silurian sections in the world. This widespread sequence of epicontinental carbonates and calcareous shales lies on the southwestern edge of the Russian Platform and contains most of the facies and ecological associations characteristic of marginal basins. The essentially undeformed Silurian sequence is approximately 265 m thick and is nearly complete from the Upper Llandovery (Telychian) through the Prídolí. Because of the excellent paleontological control, abundant exposures, and stratigraphic completeness, the Silurian succession in Podolia was proposed as a candidate for the Silurian-Devonian boundary global stratotype (Koren' et al. 1989). As a consequence, numerous biostratigraphic and lithostratigraphic investigations have been conducted producing one of the best-documented Silurian successions in the world (Koren' et al. 1989; Drygant 1983; Nikiforova 1977). In the course of these investigations approximately two dozen K-bentonite beds were recognized and detailed measurements were made of their stratigraphic positions and distribution in order to maximize their potential for local correlation (Tsegelnjuk 1980a, 1980b). Their correlative usefulness throughout the basin, and their potential equivalence with altered ash beds of similar age in Gotland, Great Britain, Poland, Scandinavia, and the Czech Republic, made them important for further, detailed studies. They are also of special interest in being the southeastern-most occurrence of lower Paleozoic K-bentonites recorded in Europe, and appear to have originated from a different source area than those in northwestern Europe (Huff et al. 2000).

K-bentonite beds in late Wenlock through Prídolí strata of Podolia, Ukraine, record episodes of explosive silicic volcanism associated with an active subduction margin. Sixteen of the known twenty-four beds were studied in detail by Huff et al. (2000) (**Figure 15**). The dominant non-clay mineral composition of the coarse fraction consists of a characteristic volcanogenic suite of biotite, quartz, and sanidine with lesser amounts of apatite and zircon. All samples consist of regularly mixed-layer, R0 to R3-ordered I/S with the illite content varying between 18% and 95%. The non-systematic distribution of percent illite as a function of depth together with a correlative association between high illite and high K^+-containing host rocks suggests a strong facies control on clay diagenetic behavior. Whole rock immobile element chemistry of the K-bentonites suggests the source magmas were generally felsic in nature. Środoń et al. (2013) reported some samples with a relatively sharp diffraction peak between 14.1 and 14.9 Å, which may correspond to a chlorite recently weathered into a mixed-layer vermiculite/smectite. These data argue for a volcanic origin in a subduction-related setting involving the partial melting of continental crust, either as part of a magmatic arc along a plate margin or as arc volcanoes resting on fragments of continental crust and generated as a consequence of plate convergence. Evidence to date indicates that the Mid-Upper Silurian K-bentonite volcanism was associated geographically with an active subduction zone in the Rheic Ocean near the southeastern side of Baltica. The presence of calc-alkaline magmatic rocks in the late Silurian and early Devonian rocks of Scotland further suggest that subduction continued westward along the margin of the Rheic Ocean during that time (Huff et al. 2000).

Nova Scotia

Silurian (Llandoverian) K-bentonites from Nova Scotia, eastern Canada were described by Bergström et al. (1997a). A remarkably complete Silurian succession is exposed along the northern coast of Nova Scotia at Arisaig, about 25 km northwest of Antigonish (**Figure 16**). The area was mapped and its geology described by Boucot et al. (1974), who judged the region to have "the most continuous and best exposed sections of marine Silurian and early Lower Devonian rocks in the Appalachian Mountain system." Fieldwork in the mid 1990s led to the discovery of numerous additional Llandoverian as well as a few Ludlovian K-bentonite beds. The more than 40 separate ash beds now recognized represent the most extensive Silurian K-bentonite bed succession currently known in North America. Silurian K-bentonites are currently known from three, geographically separated groups of localities: 1) on the shore at Beechhill Cove about 3 km east of Arisaig harbor; 2) along a 0.7 km long stretch of shore exposures between the former outlet of Arisaig Brook and

French Brook southwest of Arisaig harbor; and 3) on the shore at the outlet of McAdam Brook about 1.7 km west of French Brook. Those at Beechhill Cove occur in the lower member of the Ross Brook Formation, whereas those southwest of Arisaig harbor are in the middle and upper members of the same formation, and those at McAdam Brook in the lowermost portion of the McAdam Brook Formation. Because several additional, very thin and laterally discontinuous ash beds have been observed in the long series of outcrops southwest of Arisaig harbor, it seems likely that the total number of K-bentonite beds at Arisaig exceeds 50.

As is common for many Paleozoic K-bentonites, powder XRD scans indicated that all beds are characterized by interstratified I/S with ordering ranging from Rl.5 (short-range ordered interstratification) to R3 (long-range ordered interstratification) (Moore & Reynolds 1997). Nb and Y are generally considered to be among the most alteration independent of the immobile trace elements and were found by Pearce et al. (1984) to be particularly effective in discriminating between volcanic arc and within-plate granites. Y is more abundant in ocean ridge and within-plate granites compared with volcanic arc granites, whereas Nb is particularly enriched in within-plate granites. Within-plate magmas are assumed to have been derived from upper mantle sources where enrichment of Nb (and Ta) is related to the genesis of ocean island type basaltic magmas (Weaver 1991). Arisaig K-bentonites fall almost entirely in the within-plate field, although two Llandoverian samples have relatively low Nb and Y values, placing them in the volcanic arc or syn-collision granite field (**Figure 17**).

The stratigraphic distribution of Llandoverian K-bentonite beds exhibits some similarity between Arisaig and northwestern Europe with concentrations of beds in the *sedgwickii* graptolite Zone and the presence of only a few beds in the *griestoniensis* Zone. K-bentonite beds of probable *sedgwickii* Zone age occur in North America and have been described from sites in Illinois and Manitoulin Island, Ontario (Bergstrom et al. 1992). Furthermore, recently discovered K-bentonites in the southern Appalachians (Bergstrom et al. 1998a), which are still not dated precisely, may well be of this age. The early Ludlovian (*nilssoni* Zone) K-bentonite beds at Arisaig appear to be in the same stratigraphic position as several beds recorded from Gotland (Laufeld and Jeppsson 1976). The geographic distribution of Llandoverian K-bentonites in northwestern Europe, as well as the thickness trend of the Osmundsberg K-bentonite bed, suggests a source area in the region between the present Baltoscandia and easternmost Canada. This source area was located considerably farther to the north than that of the Middle Ordovician K-bentonites (Kolata et al. 1996). However, the latter may have been relatively close to the postulated source area for the K-bentonites at Arisaig and in the southern Appalachians. Trace and major element geochemical data indicate Llandoverian through Ludlovian K-bentonites in southern Great Britain were derived from siliceous, subalkaline magmas of largely dacite to rhyolite composition. These magmas were, for the most part, calcalkaline in character and erupted in subduction-related, plate margin to ensialic margin settings. Although there is currently no consensus on the precise timing and style of collision events associated with the closing of Iapetus and the joining of eastern Avalonia, Baltica, and Laurentia, the nature and distribution of Silurian K-bentonites provide strong evidence leading to three conclusions: 1) their source was plate margin, subduction related volcanoes; 2) their explosivity continued unabated from early Llandoverian through Ludlovian time with sufficient repetitiveness and energy to leave abundant stratigraphic records throughout northwestern Europe and parts of eastern North America; and 3) if the proposal of at least two separate source areas for volcanic ash proves to be correct, it is evident that this volcanic activity was not restricted to only a limited segment of the Laurentian margin in the western Iapetus. Previous studies have concluded that Avalonia collided with Baltica in early Ashgillian times but that marine deposition in the Southern Uplands trench continued well into the Silurian.

Southern Appalachians

Subsequent work by Bergström et al. (1998a) revealed the occurrence of Silurian K-bentonites in eastern Tennessee at Thorn Hill, a well-known locality on Clinch Mountain. The Llandoverian portion of this succession, which is about 71 m thick and consists of shallow-water sandstones, siltstones, and shales, is referred to the Clinch Formation (Schoner 1985; Dorsch and Driese 1995). This unit includes two members, the 15 m thick Hagan Member, which is overlain by the 56 m thick Poor Valley Ridge Member. The lower part of the latter contains a series of K-bentonite beds, which were estimated to be about 15–25 m above the base of this member. Further study led to the discovery of four additional Llandoverian K-bentonite localities distributed over a more than 500 km long stretch of the Appalachians from northern Georgia to central Virginia.

Devonian K-bentonites

Eastern North America

Volcanic eruptions associated with the collision of Laurentia and Avalonia deposited multiple volcanic ashes, later altered to illite or I/S clay-rich K-bentonites in the adjacent Appalachian foreland basin during the Acadian Orogenic event (Dennison and Textoris 1978; Ver Straeten 2004). Lower to Middle Devonian aged sediments within the Appalachian Basin were deposited in both deep and shallow marine environments and thus represent a variety of sedimentary environments. This succession of strata in the Appalachian foreland basin feature approximately 80 thin K-bentonites. The distribution pattern of K-bentonites through the Lochkovian to Eifelian Stages (representing ˜ 30 Ma) shows a distinct pattern of clustered multiple beds, several scattered beds, and thick intervals with no K-bentonites. Four clusters of 7 to 15 individual, closely spaced layers occur in the middle Lochkovian (Bald Hill K-bentonites, Kalkberg – New Scotland Formations), late Pragian or early Emsian (Sprout Brook K-bentonites, Esopus Formation) and early Eifelian (Ver Straeten 2004) (**Figure 18**). The Tioga K-bentonites constitute the best-known, widespread, sedimentary accumulation of tephra in middle Devonian rocks of the

Appalachian Basin (Dennison and Textoris 1978). Collinson (1968) identified the stratigraphic position of the Tioga K-bentonites in the subsurface from geophysical logs in more than one hundred wells in Illinois, Iowa, and southwestern Indiana. Becker (1974) traced the Tioga K-bentonites on geophysical logs from 60 wells in southwestern and west-central Indiana, and he obtained a single sample from one of the beds from a core in Gibson County, IN (Droste and Vitaliano 1973).

As with many Phanerozoic K-bentonites, detailed examination of these Devonian K-bentonites and associated tuffs shows that in many cases they do not represent a single eruption. Multilayered and often graded beds, fossil layers within beds, the presence of authigenic minerals such as glauconite and phosphate nodules, subjacent hardgrounds, and an irregular distribution of beds through space and time raise questions about the depositional history and preservation potential of volcanic tephra in marine environments and the degree to which the beds represent a primary record of explosive volcanism. These and other lines of evidence indicate that post-depositional physical, biological, and geochemical processes (e.g., sedimentation rate, event and background physical processes, burrowing) have modified the primary record of these water-laid ash fall events. These factors may lead to preservation of primary ash deposits or to their re-sedimentation and to partial or complete mixing with background sediments. However, it is clear that the result of very detailed work by Ver Straeten (2004) and others argue convincingly that the middle Lochkovian, early Emsian, and early Eifelian were times of peak volcanic activity in eastern North America, related to times of increased tectonism in the Acadian orogen.

Carboniferous Tonsteins

Volcanic tephra that falls into marine settings commonly alters to smectitic deposits known as bentonites, the volcanic origin of which has been recognized for many decades. However, tephra falling into nonmarine coal-forming environments generally alters to kaolinitic claystones called tonsteins, and these beds have only recently been universally accepted as being volcanic in origin. The recognition of tonsteins as altered tephra is based on mineralogy, texture, radiometric age, and field relations (Bohor and Triplehorn 1993). Burial diagenesis of bentonites frequently involves the progressive illitization of a precursor smectite resulting in mixed-layer K-bentonites. Kaolinite is unstable at higher diagenetic levels, as recorded by a number of authors (e.g. Anceau 1992), who noted that in tonsteins when the volatile matter in the associated coals was above 10% kaolinite was dominant, but when the volatile matter fell below 8%, signifying higher rank, kaolinite had been replaced by illite and subsidiary Al-rich chlorite (sudoite). This conversion is not isochemical, and potassium is essential for the transformation.

There is also the possibility that illite could be a primary product in the alteration of a volcanic ash. Based on detailed petrographic work (Bouroz et al., 1983) confirmed the dominance of 1 M illite in some tonstein samples, with only a trace of kaolinite and in some cases little trace of mixed-layers within the illite. Similarly, Admakin (2002) describes tonsteins from the lower part of the Jurassic Cheremkhovo Formation in the Irkutsk Basin in southeastern Siberia where diagenetic alteration has transformed some of the kaolinite-rich beds to dominantly illite and chlorite.

Tonsteins occur on almost every continent, but are best known from Europe and North America (Lyons et al., 1994) (**Figure 19**). Their geologic range is coincident with that of coal-forming environments; i.e., from Devonian to Holocene. They most commonly occur in Late Carboniferous (Pennsylvanian) coal-bearing strata (e.g. Price and Duff, 1969), but Permian tonsteins have been described by Dai et al. (2011) and by Zhou et al. (2000), and Late Paleocene tonsteins have been reported from the Himalayan Foreland Basin (Siddaiah and Kumar 2008), and from south central Alaska (Triplehorn et al. 1984). The coal-forming environment is well suited for preservation of thin air-fall deposits because it features low depositional energy, topographic depression, rapidity of burial by organic matter, and lack of detrital input due to the baffling effect of plant growth. In the

UK coal basins two types of tonsteins based on illite content have been described (Spears, 2012): (1) tonsteins (< 10% illite) and (2) transitional tonsteins (> 10% illite). The latter consist of less kaolinite and more quartz, which reflects a greater influence of non-volcanic detritus (Strauss, 1971). Volcanic ashes deposited within or beneath peat beds are strongly affected by humic and fulvic acids generated from organic matter. This acidic, organic-rich, highly leaching environment is partly responsible for the alteration of volcanic glass and mineral phases into kaolinite by first-order (solution-precipitation) reactions. Bed thickness also affects ash alteration, resulting in a vertical zonation of clay mineralogy in thick beds. In addition, voluminous ash falls can have an important effect on the biological and hydrological regimes of the peat swamp.

Most distal tonsteins contain a restricted suite of primary volcanic minerals, such as euhedral betaform quartz, sanidine, zircon, biotite, rutile, ilmenite, magnetite, apatite, allanite, and other accessory minerals specific to a silicic magma source. Textural features indicating a volcanic air-fall origin include bimodal size distribution of components, accretionary lapilli, altered glass bubble junctions, and aerodynamically shaped altered glass lapilli (Spears 2012). Radiometric dating of primary minerals in tonsteins shows that they are coeval with the stratigraphic ages of enclosing rocks. Tonstein field relations indicate a volcanic air-fall origin because they are thin, widespread, continuous layers, with sharply bounded upper and lower contacts, that often pass beyond the bounds of the swamp and are occasionally penetrated by stumps in growth position. The volcanic air-fall origin of tonsteins predicates their usefulness in many geologic studies (Triplehorn, 1990). Because they are isochronous, tonsteins can be used to vertically zone coal beds and thus provide controls for geochemical sampling, organic petrography studies, and mine planning. Regional correlations of nonmarine strata can be made with tonsteins, and intercontinental correlations may be possible. Furthermore, the presence of clay-free volcanic-ash layers in coal beds may indicate a raised-bog origin for the peat swamp. Radiometric dating of primary volcanic minerals in tonsteins allows age determination of coal beds and the calibration of palynomorphic zones. Multiple tonsteins in thick coal beds may be useful for studying the style and history of explosive volcanism. The Pennsylvanian Fire Clay tonstein is described by Lyons et al. (2006) as a kaolinized, volcanic-ash deposit that is the most widespread bed in the Middle Pennsylvanian of the central Appalachian basin. It occurs in Kentucky, West Virginia, Tennessee, and Virginia. A concordant single-crystal U–Pb zircon datum for this tonstein gives a $^{206}Pb/^{238}U$ age of 314.6 ±0.9 Ma (2σ). This age is in approximate agreement with a mean sanidine plateau age of 311.5 ±1.3 Ma (1σ, n = 11) for the Fire Clay tonstein.

And as a segue into the Permian, Simas et al. (2013) described a light gray tonstein claystone bed, approximately 10 cm thick, that is laminated to massive, fossiliferous and interbedded within one of the upper coal seams in the Faxinal Coalfield, which is located along the southeastern outcrop belt of the Río Bonito Formation of the Paraná Basin, southern Brazil. The tonstein bed is exposed along the cut banks of the open pit and displays mostly sharp lower and upper boundaries. The mean ages of 290.6 ±1.5 Ma obtained by U-Pb SHRIMP zircon dating of tonsteins from the Faxinal coalfields show that coal generation in coalfields of the southern Paraná basin is constrained to the Middle Sakmarian. The potential source for the tonsteins of the Río Bonito Formation is thought to be related to volcanic activity in the Choiyoi Group in the San Raphael Basin, Andes.

Permian K-Bentonites

West Texas

A series of K-bentonite beds have long been recognized throughout the Middle Permian (Guadalupian) strata of Guadalupe Mountains National Park, which also contain one of the most frequently studied carbonate margins in the stratigraphic record. The designation of the Global Stratotype Sections and Points (GSSP) for the three stages of the Guadalupian Series at Guadalupe

Mountains National Park has increased interest in using these important deposits to address a wide range of geologic questions. As a result, a number of recent studies of K-bentonites that occur in outcrops and roadcuts in the Guadalupian type area have identified K-bentonite beds and potential K-bentonite beds in each stage of the Guadalupian, with the majority being present in the Middle Guadalupian (Wordian) Manzanita Member of the Cherry Canyon Formation (**Figure 20**). Two of these are present within Guadalupe Mountains National Park at Nipple Hill, which serves as both the type locality for the Manzanita Member and the location for the Late Guadalupian (Capitanian) boundary GSSP in the overlying Pinery Limestone Member of the Bell Canyon Formation. At least one additional bed is present in the Wordian section, occurring in the South Wells Member of the Cherry Canyon Formation. A new potential K-bentonite is recognized in the Early Guadalupian (Roadian) Brushy Canyon Formation southwest of Salt Flat Bench. In the Capitanian, at least one K-bentonite occurs in the Rader Member of the Bell Canyon Formation at a locality in the less frequently studied southwestern portion of Guadalupe Mountains National Park. A second potential bed is present at a locality in Bear Canyon, although it occurs in sandstone of the Bell Canyon Formation, approximately 2 meters below the base of the Rader Member. The Manzanita Limestone Member is the uppermost of three named carbonate units within the basinal Cherry Canyon Formation. Carbonate portions of the member are dominated by lithologies ranging from mudstone to fine-grained packstone (Hampton 1989; Diemer et al. 2006). A transition from dolostone to limestone occurs roughly 20 km from the basin margin (King 1948; Newell et al. 1953; Hampton 1989), though unaltered limestone remains present at the top of the member in some sections. Siliciclastic intervals are present and consist of very fine-grained quartz sandstones and siltstones (Hampton 1989). Due to the paucity of index fossils, direct biostratigraphic data from the Manzanita are difficult to obtain, although this member is well constrained to the Wordian based on its position below the GSSP of the Capitanian at Nipple Hill.

Analyses conducted on several of the Manzanita Member K-bentonites, show apatite, biotite, and zircon to be the dominant phenocryst phases, while the clay mineral assemblage is comprised of mixed-layered I/S and/or chlorite/smectite, with discrete phases of chlorite, kaolinite, and illite present in some samples. Whole rock and phenocryst geochemical data indicate the K-bentonites were derived from a calc-alkaline series magma at a destructive plate margin. These data are consistent with the suggestion by King (1948) that the Las Delicias volcanic arc in northern Mexico is the source of the parent ash. Samples were collected from bentonites at five field localities and one core, including Nipple Hill, which is the site of the Capitanian GSSP (**Figure 21**). Apatite phenocrysts from these samples were analyzed for minor, trace, and rare earth element chemistry using electron microprobe techniques. Results indicate the presence of three patterns or trends of data that are repeated at multiple localities. These groups of data are interpreted to represent coeval deposits and are correlated between several localities to form a tephrochronologic framework. This framework links Nipple Hill with several other Guadalupian type area localities.

The trace element chemistry of individual apatite grains (~30 per sample) from several bentonites was determined using electron microprobe analysis. These bentonites were collected from Manzanita Limestone localities in and near Guadalupe Mountains National Park (GMNP) and from a suspected Manzanita locality approximately 33 km into the Delaware Basin and were studied in detail by Nicklen et al. (2007). Two bentonites occur at one of these localities, Nipple Hill in GMNP. This is particularly significant because Nipple Hill serves as both the type locality for the Manzanita Limestone, as well as the Late Guadalupian (Capitanian) GSSP in the Pinery Limestone Member of the overlying Bell Canyon Formation. A second locality is a roadcut in the nearby Patterson Hills. This roadcut contains all four of the bentonites recognized in the Manzanita, and was used to assess whether the trace element chemistry of the apatite phenocrysts could be used to differentiate between multiple beds occurring in stratigraphic succession.

Figure 22 presents apatite phenocryst chemistry from the five bentonites (labeled B-1 through B-5) sampled at the Patterson Hills road cut, as Mg-Mn-Ce/Y and Mg-Mn-Cl trivariate diagrams (Nicklen et al. 2007). These elements were chosen because they proved to be the best for discriminating the apatites from these bentonites in a series of bivariate plots by electron microprobe. In both plots, each bentonite appears to have a unique grouping of data points, with samples B-4 and B-5 having noticeably higher Cl wt % and Ce/Y ratios. The remaining three samples are differentiated primarily by their Mg and Mn concentrations, although subtle variations in Cl content and Ce/Y ratios are present. There is some overlap among the samples, but each has what appears to be a unique cluster or trend of data. The two samples that show the most similarity in the various bivariate and trivariate diagrams examined are B-4 and B-5. While this figure seems to clearly show that the two samples are not completely indistinguishable, there is enough overlap in data to suggest that they may share some components. The Mg-Mn-Cl diagram shows what appear to be two groups for B-4, with one having higher Cl values that plot with B-5. As it only takes one element to discriminate between samples, it can be said that despite the overlap seen in bivariate and trivariate diagrams, the B-4 and B-5 apatites have chemical compositions that are statistically different. Results indicate that apatite grains from individual bentonites within the Manzanita have distinct trace element chemistries, allowing for correlation of beds between localities. The two bentonites from Nipple Hill have apatite trace element chemistries that match the lowest two bentonites from the Patterson Hills roadcut and are interpreted as being correlative. This interpretation is extended to the single bentonite from the suspected Manzanita locality, as its trace element chemistry matches that of the upper Nipple Hill and second lowest roadcut bentonites.

To date, only one radioisotopic date (Bowring and Erwin 1998a) has been determined for the Guadalupian, and reports of its stratigraphic position (e.g. Bowring and Erwin 1998a; Glenister et al. 1992) have been inconsistent. To address the lack of temporal control for this interval Nicklen

(2011) calculated new isotope dilution thermal ionization mass spectrometry (ID-TIMS) U-Pb ages for zircons from K-bentonites collected in the Guadalupian type area at Guadalupe Mountain National Park. A sample was collected from an 18 cm, apple-green bentonite in the Rader Limestone in the Patterson Hills. Approximately 100 crystals were separated from a ~500 ml bulk bentonite sample. Zircon crystals averaged 110 μm in length and 28 μm in width. Due to the low amounts of radiogenic lead in individual zircons crystals that resulted in short mass spectrometer runs, it was difficult to obtain reliable analyses for this sample. Preliminary results from four concordant analyses yielded a mean $^{206}Pb/^{238}U$ age of 262.58 ±0.45 Ma. Another sample was collected from a 5 cm, dark green bentonite below the South Wells Limestone in a drainage area referred to locally as Monolith Canyon. Approximately 100 crystals were separated from a ~500 ml bulk bentonite sample. Eight preliminary concordant single crystal analyses yielded a mean $^{206}Pb/^{238}U$ age of 266.50 ±0.24 Ma. The calculation of new U-Pb ID-TIMS dates in the Guadalupian type area indicate the need for changes to the geologic time scale and the temporal relationships of global events. As Nicklen (2011) points out, an age estimate of 263.5 Ma for the base of the Capitanian Stage is made based on a bentonite in the lower half of the stage defining the *J. postserrata* conodont zone dated at 262.5 Ma. This means the age of the Wordian-Capitanian boundary is younger than estimated in recent time scales. It also decreases the duration of the Capitanian to ca. 4 myr and provides a maximum age estimate for the globally correlatable Kamura cooling event. The mass extinction that has been interpreted to occur within this event is one conodont zone above the dated bentonite and therefore no older than 262.5 Ma. The new radioisotopic date from below the South Wells Limestone provides an age estimate of 266.5 Ma for the globally correlatable Illawarra reversal. It also further supports the suggestion that the existing Guadalupian radioisotopic age of 265.3 ±0.2 Ma, should be placed in the Manzanita Limestone, rather than a point nearer to the base of the Capitanian. Although it is less certain than the basal Capitanian shift, the Roadian-Wordian boundary might also be younger than current estimates.

Australia

Thompson and Duff (1965) reported K-bentonites in the Upper Permian sequence exposed on the eastern flank of the Springsure-Serocold Anticline, Bowen Basin, Queensland, Australia. The outcrop was described as containing light-colored "soapy" clay beds in a stratigraphic unit that previously had been called the Bandanna Formation. The lower part of the Bandanna Formation was subsequently re-named the Black Alley Shale. Thompson and Duff (1965) described the claystone beds of the Black Alley Shale as containing crystal-vitric tuffs and volcanic dust that was partly altered to montmorillonite. Powder diffraction analyses by Uysal et al. (2000) concluded that interstratified I-S is the dominant clay mineral in most samples. Three types of I/S were observed: 1) I/S observed mostly from the Baralaba Coal Measures in the southern Bowen Basin display randomly interstratified (R0) I/S. These clays contain <55% illite layers in I/S; 2) The second type of I-S is common from the northern part of the Bowen Basin, and it is characterized by a superstructure reflection at 26-28Å. These clays are (R1) I/S and contain 65-85% illite layers; 3) The third type of I/S is R3. These clays show asymmetrical peaks at ~9.8Å, with a broad shoulder near 11Å when glycolated.

China

Guadalupian K-bentonites from Sichuan Province have been reported by a number of authors. A recent study by Deconinck et al. (2014) describes the clay assemblages as being composed of I/S mixed-layers in altered tephra layers intercalated in the carbonate succession. The highest smectite percent was observed in the 2 m-thick Wangpo Bed and in the thickest K-bentonite (15 cm) whereas other levels have a thickness ranging only from 1 to 7 cm. The lowest smectite percent found in the K bentonites studied ranges from 6 to 16%, suggesting that the temperature reached by the sediments was close to 180° C (Środoń et al. 2009). Detrital and authigenic volcanogenic clay minerals have been partially replaced through illitization processes during burial, raising questions about diagenetic effects. K-bentonite horizons in the Wuchiaping, Dalong and Feixianguan Formations were studied in some detail, and using the I/S ratios as a measure of thermal history the authors concluded that the Permian sediments underwent burial to a depth of about 6000 m. However, kaolinite was also detected in the Wangpo bed, suggesting a detrital rather than an authigenic origin for some portions of the layer. Deconinck et al. (2014) suggested that the Wangpo bed should be considered as a reworked bentonite formed by the accumulation of volcanic ash transported from ash-blanketed local land areas into marine environments. Such epiclastic deposits are characterized by their multi meter thickness, as it is the case for the Wangpo Bed, and by the mixture of volcanogenic and detrital particles.

Brazil and South Africa

Permian bentonite beds in Brazil and South Africa record episodes of silicic explosive volcanism. Despite their distance from each other today, present day Brazil and South Africa were proximal to each other during the Permian along an active subduction zone, suggesting that volcanism in the area would likely be common. A long-standing questions is whether ash beds can be correlated between the presumably coeval Whitehill Formation of the Ecca Group in South Africa and the Late Permian (Tatarian) Irati Formation in Brazil using chemical fingerprinting, to indicate a similar source. Multiple smectite-rich bentonite beds are present in the Lower Permian Irati Formation of Southeastern Brazil, as exposed in the Petrobras Corporation's SIX Quarry, near Sao Mateus. The Irati Formation, thought to have been deposited in a hypersaline basin, is a sequence of gray shales and black oil shales interbedded with dolomite. The shales bear abundant phosphatized remains of Mesosaurid aquatic reptiles. Multiple horizons of thin (1-2 cm) gray clay beds were investigated; three beds exposed in the SIX quarry and one from a core in an area being prospected by Petrobras. Lack of large phenocrysts demonstrates that the bentonites are clearly distal, yet outcrop study points to the exotic origin of the bentonites. SHRIMP analyses performed by Santos et al. (2006) on the euhedral and prismatic grains revealed an age of ca. 278.4 ±2.2 Ma and are interpreted as the crystallization age of the volcanic eruption. Based on this new dating, the Irati Formation was reassigned to the Lower Permian (Cisuralian), Artinskian in age, modifying the Late Permian ages previously attributed to this unit.

Black shale is the dominant facies of both formations (**Figure 23**), with the Irati having more organic matter. In an experimental study of both the Irati and Whitehill Formation K-bentonites (Sylvest et al. 2012), the samples analyzed were distal to the volcano of origin as confirmed by the lack of phenocrysts in all samples. Initial research was done with X-ray diffraction (XRD) in order to determine clay composition of the samples. Mixed layer clays were found in both South Africa and Brazil, but the compositions differed. Samples from South Africa contained mixed-layer I/S, whereas samples from Brazil contained mostly smectite, with some kaolinite. The difference in clays is due to differing post-depositional histories. Brazilian samples containing kaolinite underwent more chemical weathering than samples taken from drier South Africa. In order to determine concentrations of major and trace elements, X-ray fluorescence (XRF) was used to analyze select samples. Data from XRF using Nb/Y and Zr/TiO_2 indicated a complete overlap between the Irati and all of the Ecca Group (Collingham, Whitehill and Prince Albert) Formations, signifying a similar dacitic and rhyolitic source. There is a separation of the end member tephras into dacitic and rhyolitic groups, and both groups are present in all of the stratigraphic units. TiO_2/Zr vs. Nb/Y discrimination diagrams indicate the parent volcanic ash was rhyolitic in nature. Rare Earth Element (REE) analysis was conducted on each of the bentonite beds and also on adjacent shale samples. LREE enrichment and a negative Eu anomaly indicates that the parental magma was felsic. REE analysis also reveals that the shales contain a volcanic component. The

REE data of these K-bentonite beds was used for correlation with coeval Late Permian strata in Southern Africa (Maynard et al. 1996).

Elliot and Watts (1974) described ash fall tuff horizons in many boreholes and outcrops from the Permian Ecca and Beaufort Groups in South Africa. Rubidge et al. (2013), in a study of K-bentonites associated with vertebrate fossil horizons in the Beaufort Group, found that their geochronologic results established the following age constraints for the Beaufort vertebrate assemblage zones and, by correlation, for the Middle to Late Permian tetrapod-bearing Pangean deposits: 261.24 Ma for the lower-middle *Pristerognathus* Zone (equivalent to the *Jinogondolella xuanhanensis* conodont Zone), 260.41 Ma for the upper *Pristerognathus* Zone (equivalent to the *Jinogondolella granti* conodont Zone), 259.26 Ma for the *Tropidostoma* Zone (equivalent to the *Clarkina postbitteri* conodont Zone), 256.25 Ma for the early-middle *Cistecephalus* Zone (equivalent to the *Clarkina transcaucasica* conodont Zone), and ca. 255.2 Ma for the top of this biozone (equivalent to the *Clarkina orientalis* conodont Zone). They concluded that there was no correlation between vertebrate extinctions in the Karoo Supergroup and the marine end-Guadalupian mass extinction. Martini (1974), McLachland and Jonker (1990), Fildani et al. (2009), Wilson and Guiraud (1998) and the majority of authors interested in the matter, agree that the sources for the African tuffaceous units were most likely located in Patagonia and/or West Antarctica. Dos Anjos et al. (2010) suggest that the probable source of the Irati ash was the Choiyoi Province, a calc-alkaline magmatic arc developed between 275 and 250 Ma in southern Gondwana. The somewhat more andesitic bentonites beds that occur in the Whitehill and Prince Albert Formations in the Main Karoo basin, South Africa are suggested by Dos Anjos et al. (2010) to have had a slightly different source. However, data reported by Sylvest et al. (2012) strongly suggests the two successions were affected by the same volcanic source (**Figure 24**).

Four deglaciation sequences recorded in the Dwyka Group of Namibia and South Africa are capped by mudstone units such as the 45 m thick marine fossil-bearing Ganigobis Shale Member in Namibia in which 24 thin ash fall horizons are preserved (Bangert et al. 1999). Ion microprobe analyses of magmatic zircons from the tuff horizons yielded a new radiometric age calibration of the top of deglaciation sequence II and of the Dwyka/Ecca Group boundary in southern Africa of 302.0 ±3.0 Ma and 299.2 ±3.2 Ma (latest Kasimovian) for the top of DS II. Juvenile zircons from two tuff horizons of the basal Prince Albert Formation, sampled north of Klaarstroom and south of Laingsburg in the Western Cape (South Africa), were dated at 288.0 ±3.0 and 289.6 ±3.8 Ma (earliest Asselian). According to these age determinations, the deposition of Dwyka Group sediments in southern Africa started by the latest at about 302 Ma and ended at about the Carboniferous - Permian boundary, 290 Ma before present (Bangert et al. 1999). And similarly, U-Pb ages determined on single-grain zircons from 16 ash beds within submarine fan deposits of the Ecca Group provide the first evidence of a marine Permian-Triassic (P-T) boundary in the Karoo Basin of South Africa (Fildani et al. 2009).

Uruguay

Permian bentonite beds have been described in different geological formations of the South East part of the Paraná Basin, including the Rio do Rastro area in Acegua, Brazil, Tuñas and Yaguari Formations, in the Sierras Australes, Argentina and the Bañado de Medina-Melo area, Uruguay (Calarge et al. 2006). A >2 m thick Permian bentonite bed that occurs in the Melo, Uruguay area is composed of an exceptionally well-crystallized Ca-montmorillonite (Calarge et al. 2003). Compaction during burial has made the bentonite bed a K-depleted closed system in which diagenetic illitization was inhibited. This bentonite bed and the Acegua one belong to the Late Permian Yaguary Formation (Tatarian). The succession consists mainly of sandstones of fluvial and eolian origin alternating with mudstone deposits, which are generally considered to be lagoonal deposits formed during the Late Permian regression. The preservation of smectite pseudomorphs of glass shards in the upper sandstone confirms that volcanic ashes were deposited into low energy environments where current sorting and redistribution were minimal. Changes in major and trace element content with depth suggests that the Melo bentonite bed likely resulted from the superposition of two different volcanic ash deposits that occurred sufficiently close together in time so that no lacustrine sedimentation was preserved between them.

Triassic K-bentonites

The Chinle Formation, widely exposed throughout the Colorado Plateau area, was deposited in a large basin that was filled by westward and northwestward flowing streams and lacustrine sediments (Blakey and Gubitosa 1983). According to Smiley (1985), the Mogollon highlands, situated within central and southern Arizona, provided a source of eolian and fluvial-transported volcanic sediments, lahars and sediments from the older Permian-age formations. Within southeastern Utah, the Uncompahgre highlands are said to have provided a further source of volcaniclastic material. However, studies by Blakey and Middleton (1983) indicate that the source area for the volcaniclastics is not clearly established. At least some of the volcaniclastic material deposited by the Chinle streams was probably derived from the Cordilleran volcanic arc to the west and southwest of the Chinle basin, and other clasts in the Sonsela and Shinarump are most likely derived from Precambrian sources in central Arizona. The tectonic and depositional situation within Arizona changed within the Upper Triassic, and especially during the Triassic-Jurassic transition. Studies by Wilson and Stewart (1967) point to a decrease in volcanogenic bentonites, an increase in grain size and a sediment-color change that marks the Triassic-Jurassic boundary. Sedimentological changes also are apparent between the upper and lower Petrified Forest members, indicating changes in fluvial and lacustrine deposition and possibly as concerns tectonism and climate.

Perhaps the earliest report of tephra layers in the Chinle Formation of Arizona, New Mexico and Utah was produced by Allen (1930) who undertook a petrographic study of montmorillonite-rich beds that contained textures similar to pumice with minute elongate vesicular cavities, suggesting that the montmorillonite has formed from volcanic ash with the retention of its structure. In addition the beds included euhedral sanidine, quartz, biotite, magnetite, apatite, and zircon crystals. Above the Moss Back Member, lavender and brown variegated mudstone and sandstone of the Petrified Forest Member (Dubiel 1987) has bentonites, thin lenses of carbonate nodule conglomerate, and sandy units with large scale internal scour surfaces and large trough cross-stratification. The volcanic ash originated from a prolonged series of eruption events beginning 225 Ma. The volcanic eruptions leveled trees and the resulting ash covered the entire area and mixed with the water of the swampland to cause massive flooding and lahars (mudflows caused by an influx of volcanic ash). The volcanic ash layers are responsible for the gray base colors of the Painted Desert while the oxidation of other ash layers create the pastel reds and purples found throughout the landscape.

New Zealand

Near Kaka Point on the southeast coast of Otago, South Island, New Zealand is a Middle Triassic marine sequence of siltstones and subordinate volcanogenic sandstones, in all over 1.5 km thick. The section contains over 300 thin interbedded ash beds (Boles and Coombs 1975) and they range from a few millimeters to a few decimeters in thickness. Sedimentary structures suggest that they have been re-deposited. Three main types may be distinguished. One type is bentonitic, commonly containing crystal clasts near the base and relict heulanditized glass shards, representing yet another pathway for tephra alteration. Boles and Coombs (1975) reported that in seventeen such bentonites examined from the Triassic section in the Hokonui Hills, smectites are predominant in most samples relative to subordinate illite. Ahn et al. (1988) studied some of the beds in detail, focusing on beds that appeared to be primary air-fall tephras. The bentonite samples were collected from the Tilson Siltstone, near the top of the Etalian Stage, Middle Triassic, approximately 700 m north of Kaka Point promontory. One bed in particular is about 10-20 cm thick, with thin silty laminae containing clasts of fresh, unaltered plagioclase and quartz about 60 µm in diameter together with numerous relicts of cuspate glass shards, some reaching 0.2 mm in size. Microprobe analyses show that the feldspars are mostly An_{58-28}, with a few grains of alkali feldspar. The glass shards are largely replaced by K-rich, Si-rich heulandite ranging into clinoptilolite. The matrix contains very fine-grained aggregates of clay minerals and small cubic crystals and framboids of pyrite.

Jurassic K-bentonites

Explosive volcanic activity is recorded in the Upper Jurassic of the Paris Basin and the Subalpine Basin of France by the identification of five bentonite horizons. These layers occur in Lower Oxfordian (*cordatum* ammonite zone) to Middle Oxfordian (*plicatilis* zone) clays and silty clays deposited in outer platform environments. In the Paris Basin, a thick bentonite (10–15 cm), identified in boreholes and in outcrop, is dominated by dioctahedral smectite (95%) with trace amounts of kaolinite, illite and chlorite. In contrast, five bentonites identified in the Subalpine Basin, where burial diagenesis and fluid circulation were more important, are composed of a mixture of kaolinite and regular or randomly interstratified I/S mixed-layer clays in variable proportions, indicating a K-bentonite. In the Subalpine Basin, a 2–15 cm thick bentonite underlain by a layer affected by sulfate and carbonate mineralization can be correlated over 2000 km^2. Potassium feldspars including sanidine and microcline have been identified by SEM and by petrographic microscopy. Euhedral crystals of zircon, apatite and biotite were identified in smear slides and thin sections, but these correspond to only a minor component of the bulk rock, which is composed dominantly of clay minerals. The geochemical composition of the bentonites in both basins is characterized by high concentrations of Hf, Nb, Pb, Ta, Th, Ti, U, Y, Zr and low concentrations of Cr, Cs and Rb. Biostratigraphical and geochemical data suggest that the thick bentonite in the Paris Basin correlates with the thickest bentonite in the Subalpine Basin, located 400 km to the south. These horizons indicate that significant explosive volcanic events occurred during the Middle Oxfordian and provide potential long-distance isochronous marker beds. Immobile element discrimination diagrams and REE characteristics indicate that the original ash compositions of the thickest bentonites correspond to a trachyandesitic source from a within-plate alkaline series that was probably related to North Atlantic rifting (Pellenard et al. 2003, 2013). The thickest ash layer, attributed to the *Gregoryceras transversarium* ammonite Biozone (Oxfordian Stage), yielded a precise and reliable ^{40}Ar–^{39}Ar date of 156.1 ±0.89 Ma, which was found to be in better agreement with the GTS2004 Time Scale boundaries than with the later GTS2012 description. This first biostratigraphically well-constrained Oxfordian date was proposed as a new radiometric tie-point to improve the Geologic Time Scale for the Late Jurassic, where ammonite-calibrated radiometric dates are particularly scarce.

High-resolution sedimentological studies of Jurassic shaly formations from the Subalpine Basin (France), the Paris Basin, and the Hebrides Basin (Skye, Scotland) reveal the occurrence of bentonite layers from the Upper Callovian to the Middle Oxfordian, indicating perennial aerial explosive volcanic activity. In the field, bentonites occur as centimetric white-to-grey plastic clayey horizons interbedded in shales. They derive from the devitrification of unstable ash and volcanic dust at the seawater/sediment interface. All bentonites are composed of pure smectite or, in the case of diagenesis, a mixture of kaolinite and smectite/I-S mixed-layers. These levels are characterized by a specific geochemical signature, unlike enclosed detrital shales (Pellenard et al. 2003).

Pellenard et al. (2003) identified nine thin bentonites in the Hebrides Basin. The oldest horizon occurs in the *Athleta* biozone (Callovian, Dunans Clay Fm), the youngest appears in the *densiplicatum* biozone (Oxfordian, Glashvin Silt Fm). In the Subalpine Basin, five bentonites were identified in the Terre Noires Fm (Oxfordian) from the *cordatum* to the *plicatilis* biozones. One of these, 10-15 cm thick (*vertebrale* subzone) correlated with the only bentonite recognized in the Paris Basin, 400 km to the north, on the basis of geochemical and biostratigraphic data, constituting a key stratigraphic marker-bed. Correlations and the chemical fingerprint suggest that this thick horizon and all bentonites from the Hebrides Basin are from a single magmatic source. The Zuidwal within-plate alkaline volcanic center (Netherlands) is thought to constitute the most realistic source (Pellenard et al. 2003).

In Australia five seams of commercial-quality bentonite crop out in a scarp north of Miles in southern Queensland and another on the plain 1000 feet to the west. Bentonite in the same general interval was also intersected in shallow drill holes nearby (Exon and Duff 1968). These outcrops are part of an Upper Jurassic sequence in which the bentonites were preserved in back-swamp environments away from Jurassic stream channels, and are thought to be widespread in the Upper Jurassic sequence of the Surat Basin. And Duff and Milligan (1967) described another occurrence in the upper part of the Upper Jurassic OralIo Formation in the Yuleba area. The Miles deposit is thought to be related to the same period of volcanism as the Yuleba deposit but is somewhat older. The sediments containing this bentonite are equivalent to either the uppermost Injune Creek Group or the lowermost OralIo Formation but are not lithologically typical of either unit (Duff and Milligan 1967).

Cretaceous K-Bentonites

Bentonites are abundant throughout the Cretaceous stratigraphic sections of western and northern North America with numerous bentonite deposits characterizing the Upper Cretaceous. Thirty bentonites described from Cretaceous sections across the eastern and western Canadian Arctic, as well as the Western Interior Basin were used to evaluate the geochemical signatures of volcanism over space and time (Dixon et al. 1992). And in the Lower Cretaceous of the Peace River coalfield the X-ray diffraction analysis of 75 thin volcanic clay bands shows kaolinite and mixed-layer I/S to be the two clay minerals present. Kaolinite is dominant in the clay bands (tonsteins) in the coal-bearing Gething and Gates formations, whereas I/S is dominant in the K-bentonite clay bands in the marine Moosebar Formation. A complete gradation exists between the two clay minerals, demonstrating their common volcanic origin (Spears and Duff 1984).

As another example, the Late Cretaceous Niobrara Formation and Pierre Shale Group are exposed throughout western Kansas, Wyoming, Montana and South Dakota, and contain numerous bentonite beds formed as a result of the subduction of the Farallon Plate along the western margin of North America (DeCelles 1994). As an example, the Sharon Springs Formation in the Pierre Shale Group contains the Ardmore bentonite succession, with individual beds up to 1 m in thickness. The distribution of the bentonites can be used to for regional correlation of units in the lower Pierre Shale. Bentonites of the Gammon Ferruginous Member in the Black Hills correlate with bentonites of the organic-rich shale unit in western Kansas, although the interval is not present in central and eastern South Dakota or North Dakota. Bentonites of the Ardmore bentonite succession are present in the Black Hills, central & eastern South Dakota and North Dakota, however (Bertog et al. 2007). Beyond these descriptions, an excellent summary of Cretaceous and Tertiary bentonites is provided by Grim and Güven (1978).

Summary

Detailed field and laboratory studies of K-bentonites, bentonites and tonsteins provides an excellent set of tools for the interpretation of topics such as regional stratigraphy, paleovolcanism, tectonic reconstruction, weathering and diagenesis. Questions frequently arise as to whether a particular clay-rich bed might be an altered volcanic ash fall in the form of a bentonite or K-bentonite. These beds are often datable using fission track and U/Pb dating of zircons plus K/Ar and Ar/Ar dating of amphibole, biotite and sanidine. Due to their unique composition, these deposits provide an indispensable tool when correlating sections. The criteria for recognizing such beds are varied, but fall into the two broad categories of field criteria and laboratory criteria. Ideally, one would want information from both, but often that is not possible. However, there are key features to look for in each case that can aid in reliable identification. Field criteria: K-bentonites can be different colors when wet (blue, green, red, yellow) but are characteristically yellow when weathered. Due to their clay rich nature, they will feel slippery and waxy when wet. Some K-bentonites contain euhedral to anhedral volcanogenic biotite, quartz, feldspar, amphibole, zircon and apatite. The typical appearance of a K-bentonite bed in outcrop is that of a fine-grained clay-rich band ranging between 1 mm – 2 m in thickness that has been deformed by static load from the enclosing siliciclastic or carbonate sequence. Accelerated weathering of K-bentonites causes them to be recessed into the outcrop face. For thicker K-bentonites there is often a zone of nodular or bedded chert in the adjacent strata at both the base and the top of the bed. Laboratory criteria: Most bentonites and K-bentonites are smectite- or I/S-rich, although some may contain a considerable amount of kaolinite, and those that have undergone low-grade metamorphism may be dominated by R3 I/S or sericite, or both, plus interstratified chlorite/smectite (corrensite) and/or chlorite. These deposits have formed throughout Earth's history because explosive volcanic activity has played an important role in the evolution of our planet. However, only those formed after the Jurassic, and especially those in the Cenozoic, have economic importance. Nevertheless, older altered tephras, in which smectite has converted to mixed-layer I/S, are important stratigraphic markers used for correlation purposes.

Acknowledgements

In addition to the many colleagues, particularly Dennis Kolata and Stig Bergström, and students without whose collaborative work over the years this report would not be possible, I would like to express my deep appreciation for the very thoughtful and constructive reviews provided by Alain Meunier and Chuck Ver Straeten, as well as to Rich April for his great attention to detail as Associate Editor in moving this manuscript through the publication process.

References Cited

Admakin, L.A. (2002) Accumulation and Post-Sedimentary Diagenesis of Tonsteins, Lithology and Mineral Resources, 37 (1), 60–67.

Ahn J.H., Peacor D.R., and Coombs D.S. (1988) Formation mechanisms of illite, chlorite and mixed layer illite-chlorite in Triassic volcanogenic sediments from the Southland Syncline, New Zealand. Contributions to Mineralogy and Petrology, 99, 82-89.

Allen, V.T. (1929) Altered Tuffs in the Ordovician of Minnesota, Journal of Geology, 37, 239-248.

Allen, V.T. (1930) Triassic bentonite of the Painted Desert, American Journal of Science, Series 5, 19, 283-288.

Anceau, A. (1992) Sudoite in some Visean (Lower Carboniferous) K-bentonites from Belgium. Clay Minerals, 27, 283-292.

Astini, R.A., Collo, G., and Martina, F. (2007) Ordovician K-bentonites in the upper plate active margin of Western Gondwana, (Famatina Ranges): stratigraphic and palaeogeographic significance: Gondwana Research, 11, 311–325.

Bangert, B., Stollhofen, H., Lorenz, V. and Armstrong, R. (1999) The geochronology and significance of ash-fall tuffs in the glaciogenic Carboniferous-Permian Dwyka Group of Namibia and South Africa. Journal of African Earth Sciences, 29 (1), 33-49.

Becker, L. E. (1974) Silurian and Devonian rocks in Indiana southwest of the Cincinnati Arch: Indiana Geological Survey Bulletin 50, 83 p.

Bergström, S.M., Huff, W.D., Kaljo, D., and Kolata, D.R. (1992) Silurian K-bentonites in the Iapetus region; a preliminary event-stratigraphic and tectonomagmatic assessment: Geologiska

Foereningen i Stockholm Foerhandlingar, 114 (3), 327-334.

Bergström, S.M., Huff, W.D., Kolata, D.R. and Bauert, H. (1995) Nomenclature, stratigraphy, chemical fingerprinting, and areal distribution of some Middle Ordovician K-bentonites in Baltoscandia. GFF 117, 1–13.

Bergström, S.M., Huff, W.D., Kolata, D.R., Krekeler, M.P.S., Cingolani, C., and Astini, R.A. (1996) Lower and Middle Ordovician K-bentonites in the Precordillera of Argentina: A progress report: XIII Congreso Geológico Argentino y II Congreso de Exploración de Hidrocarburos, V, 481-490.

Bergström, S.M., Huff, W.D., Kolata, D.R., and Melchin, M.J. (1997a) Occurrence and significance of Silurian K-bentonite beds at Arisaig Nova Scotia, Eastern Canada. Canadian Journal of Earth Sciences 34, 1630–1643.

Bergström, S.M., Huff, W.D., Kolata, D.R., Yost, D.A., and Hart, C. (1997b) A unique Middle Ordovician K-bentonite bed succession at Röstånga, S. Sweden: Geologiska Föreningens I Stockholm Förhandlingar, 119, 231–244.

Bergström, S.M., Huff, W.D., and Kolata, D.R. (1998a) Early Silurian (Llandoverian) K-bentonites discovered in the southern Appalachian thrust belts, eastern USA: Stratigraphy, geochemistry, and tectonomagmatic and paleogeographic implications. GFF 120, 149–158.

Bergström, S.M., Huff, W.D., and Kolata, D.R. (1998b) The lower Silurian Osmundsberg K-bentonite. Part I: Stratigraphic position, distribution, and palaeogeographic significance. Geological Magazine 135, 1–13.

Bergström, S.M., Schmitz, B., Saltzman, M.R., and Huff, W.D. (2010) The Upper Ordovician Guttenberg $\delta^{13}C$ excursion (GICE) in North America and Baltoscandia: Occurrence, chronostratigraphic significance and paleoenvironmental relationships: In: Finney, S.C. and

Berry, W. (Eds.) Earth system during the Ordovician Period: Geological Society of America Special Paper 466, 37-67.

Bertog, J., Huff, W.D., and Martin, J.E. (2007) Geochemical and mineralogical recognition of the bentonites in the lower Pierre Shale Group and their use in regional stratigraphic correlation: In: J.E. Martin and D.C. Parris (Eds.) The Geology and Paleontology of the Late Cretaceous Marine Deposits of the Dakotas, Geological Society of America Special Paper 427, 23-50.

Blakey, R.C., and Gubitosa, R. (1983) Late Triassic paleogeography and depositional history of the Chinle Formation, southern Utah and northern Arizona. in M.W. Reynolds and E.D. Dolly (eds.) Mesozoic paleogeography of west-central United States. Rocky Mountain Paleogeography Symposium 2: Rocky Mountain Section, Society of Economic Paleontologists and Mineralogists, 57-76.

Blakey, R.C., and Middleton, L. (1983) Lower Mesozoic stratigraphy and depositional systems, southwest Colorado Plateau. Geologic excursions in stratigraphy and tectonics; from southeastern Idaho to the southern Inyo Mountains, California, via Canyonlands and Arches National Parks, Utah. Utah Geological and Mineralogical Survey Special Studies 60, 33-39.

Bohor, B.F., and Triplehorn, D.M. (1993) Tonsteins: Altered Volcanic-Ash Layers in Coal-Bearing Sequences. Geological Society of America Special Papers, 285, 44 p.

Boles J.R., and Coombs D.S. (1975) Mineral reactions in zeolitic Triassic tuff, Hokonui Hills, New Zealand. Geological Society of America Bulletin 86, 163-173.

Boucot, A.J., Dewey, J.P., Dineley, D.L., Fletcher, R., Fyson, W.K., Griffin, J.G., Hickox, C.F., McKerrow, W.S., and Ziegler, A.M. (1974) Geology of the Arisaig area, Antigonish County, Nova Scotia. Geological Society of America, Special Paper 139, 196 p.

Bouroz, A., Spears, D.A., and Arbey, F. (1983) Essai de synthese des donnees acquises sur la genese et l'evolution des marqueurs petrographiques dans les bassins houillers. Memoire XVI, Societe Geologique du Nord. 114 pp.

Bouyo Houketchang, M., Zhao, Y., Penaye, J., Zhang, S.H., and Njel, U.O. (2015) Neoproterozoic subduction-related metavolcanic and metasedimentary rocks from the Rey Bouba Greenstone Belt of north-central Cameroon in the Central African Fold Belt: New insights into a continental arc geodynamic setting. Precambrian Research, 261, 40-53.

Bowring, S.A., and Erwin, D.H. (1998a) A new look at evolutionary rates in deep time: uniting paleontology and high-precision geochronology. GSA Today, 8,1-8.

Bowring, S.A., Davidek, K., Erwin, D.H., Jin, Y.G., Martin, M.W., and Wang, W. (1998b) U-Pb zircon geochronology and tempo of the end-Permian mass extinction. Science, 280:1039-1045.

Brun, J., and Chagnon, A. (1979) Rock stratigraphy and clay mineralogy of volcanic ash beds from the Black River and Trenton Groups (Middle Ordovician) of southern Quebec: Canadian Journal of Earth Sciences, 16, 1499-1507.

Calarge, L.M., Meunier, A., and Formoso, M.L. (2003) A bentonite bed in the Acegua (RS, Brazil) and Melo (Uruguay) areas: a highly crystallized montmorillonite. Journal of South American Earth Sciences, 16 (2), 187–198.

Calarge, L.M., Meunier, A., Lanson, B., and Formoso, M.L. (2006) Chemical signature of two Permian volcanic ash deposits within a bentonite bed from Melo, Uruguay. Annals of the Brazilian Academy of Sciences, 78 (3), 525-541.

Chen, D., Wang, J., Qing, H., Yan, D., and Li, R. (2009) Hydrothermal venting activities in the Early Cambrian, South China: petrological, geochronological and stable isotopic constraints. Chemical Geology, 258, 168–181.

Cocks, L.R.M., and Torsvik, T. (2005) Baltica from the late Precambrian to mid-Paleozoic times: The gain and loss of a terrane's identity: Earth-Science Reviews, 72, 39–66.

Collinson, C. (1968) Devonian of the north-central region, United States. In: D. H. Oswald, ed., International symposium on the Devonian system, 1967, Calgary, Alberta. Proceedings 1. Alberta Society of Petroleum Geologists 1, 933-971.

Conkin, J.E., and Conkin, B.M. (1992) Paleozoic Metabonites of North America: Part 3 - New Ordovician Metabentonites from Kentucky and Tennessee: Universiy of Louisville Studies in Paleontology and Stratigraphy, 20, 1-30.

Cressman, E.R. (1973) Lithostratigraphy and depositional environments of the Lexington Limestone (Ordovician) of central Kentucky, U.S. Geological Survey, Professional Paper, 768, 61 p.

Dai, S., Wang, X., Zhou, Y., Hower, J.C., Li, D., Chen, W., and Zhu, X. (2011) Chemical and mineralogical compositions of silicic, mafic, and alkali tonsteins in the late Permian coals from the Songzao Coalfield, Chongqing, Southwest China. Chemical Geology 282, 29–44.

Dalla Salda, L., Bossi, J., and Cingolani, C. (1988) The Rio de la Plata cratonic region of southwestern Gondwanaland: Episodes, 11, 263–269.

DeCelles, P.G. (1994) Late Cretaceous-Paleocene Synorogenic Sedimentation and Kinematic History of the Sevier Thrust Belt, Northeast Utah and Southwest Wyoming. Geological Society of America Bulletin, 106 (1), 32-56.

Decker, N.B., Byerly, G.R., Thompson Stieglera, M., Lowe, D.R., and Stefurak, E. (2015) High resolution tephra and U/Pb chronology of the 3.33–3.26 Ga Mendon Formation, Barberton Greenstone Belt, South Africa. Precambrian Research, 261, 54-74.

Deconinck, J.F., Crasquin, S., Bruneau, L., Pellenard, P., Baudin, F., and Feng, Q. (2014) Diagenesis of clay minerals and K-bentonites in Late Permian/Early Triassic sediments of the Sichuan Basin (Chaotian section, Central China), Journal of Asian Earth Sciences 81, 28–37.

Dennison, J.M., and Textoris, C.A. (1978) Tioga bentonite time-marker associated with Devonian shales in Appalachian Basin, in Schott, B.L., Overbey, W.K., Jr., Hunt, A.E., and Komar, C.A., eds., Proceedings of the First Eastern Gas Shales Symposium: U.S. Department of Energy, Publication MERC/SP-77–5, 166–182.

Diemer, J.A., Tyrrell, W.W. Jr., Bell, G.L., and Griffing, D.H. (2006) A Patterson Hills Section of the Bentonite-Bearing Manzanita Limestone of the Cherry Canyon Formation, Culberson County, Texas, in Hinterlong, G., ed. Permian Basin Section SEPM, Publication 2006-46, 52-58.

Dixon, J., Dietrich, J., Snowdon, L.R., Morrel, G., and McNeil, D.H. (1992) Geology and petroleum potential of Upper Cretaceous and Tertiary strata, Beaufort-Mackenzie area, Northwest Canada. AAPG Bulletin 76 (6), 927-947.

Dorsch, J., and Driese, S.G. (1995) The Taconic foredeep as sediment sink and sediment exporter: Implications for the origin of the white quartz arenite blanket (Upper Ordovician–Lower Silurian) of the central and southern Appalachians. American Journal of Science 295, 201–243.

Dos Anjos, C.W.D., Meunier, A., Guimarães, E.M., and El Albani, A. (2010) Saponite-Rich Black Shales And Nontronite Beds Of The Permian Irati Formation: Sediment Sources And Thermal Metamorphism (Parana´ Basin, Brazil) Clays and Clay Minerals, 58 (5), 606–626.

Dristas, J.A., and Frisicale, M.C. (1987) Rocas piroclasticas en el sector suroeste de las sierras septentrionales de la Provincia de Buenos Aires. Revista de la Asociación Argentina de Mineralogia, Petrologia y Sedimentologia, 18, 33-45.

Droste, J.B., and Vitaliano, C.J. (1973) Tioga Bentonite (Middle Devonian) of Indiana. Clays and Clay Minerals, 21, 9-13.

Drygant, D.M. (1983) History of Previous Research of the Silurian of Podolia. In: B. S. Sokolov (ed.) The Silurian of Podolia. Academy of Sciences of the Ukrainian SSR, Kiev, 60-61.

Dubiel, R.F. (1987) Sedimentology of the Upper Triassic Chinle Formation, Southeastern Utah: Paleoclimate Implications. Journal of the Arizona-Nevada Academy of Science. 22, 35-45

Duff, P.G., and Milligan, E.N. (1967) Upper Jurassic bentonite from Yuelba Creek, Roma District, Australia, Bureau of Mineral Resources, Geology and Geophysics Report 9, 5p.

Elliot, D.H., and Watts, D.R. (1974) The nature of volcaniclastic material in some Karroo and Beacon rocks. Transactions of the Geological Society of South Africa, 77, 109-111.

Exon, N.F., and Duff, P.G. (1968) Jurassic bentonite from the Miles District, Queensland. Bureau of Mineral Resources, Geology and Geophysics Report 49, 20p.

Fildani, A., Weislogel, A., Drinkwater, N.J., McHargue, T., Tankard, A., Wooden, J., Hodgson, D., and Flint, S. (2009) U-Pb zircon ages from the southwestern Karoo Basin, South Africa—Implications for the Permian-Triassic boundary, Geology, 37 (8) 719–722.

Fletcher, C.J.N., Chan, L.S., Sewell, R.J., Campbell, S.D.G., and Davis, D.W. (2004) Basement heterogeneity in the Cathaysia crustal block, southeast China, in Malpas, J., Fletcher, C.J.N., Ali, J.R., and Aitchison, J.C., eds., Aspects of the Tectonic Evolution of China: Geological Society, London, Special Publication 226, 145–155.

Fortey, N.J., Merriman, R.J., and Huff, W.D. (1996) Silurian and Late Ordovician K-bentonites as a record of late Caledonian volcanism in the British Isles: Transactions of the Royal Society of

Edinburgh, Earth Sciences, 86, 167–180.

Glenister, B.F., Boyd, D.W., Furnish, W.M., Grant, R.E., Harris, M.T., Kozur, H., Lambert, L.L., Nassichuk, W.W., Newell, N.D., Pray, L.C., Spinosa, C., Wardlaw, B.R., Wilde, G.L., and Yancey, T.E. (1992) The Guadalupian: proposed International Standard for a Middle Permian Series. International Geological Review, 34, 857□888.

Grim, R.E., and Gu□ven, N. (1978) Bentonites - geology, mineralogy, properties and uses: Developments in Sedimentology, 24, Elsevier, New York, NY. 256 p.

Grotzinger, J.P., Bowring, S.A., Saylor, B.Z., and Kaufman, A.J. (1995) Biostratigraphic and geochronologic constraints on early animal evolution. Science, 270, 598-604.

Hagemann, F., and Spjeldnæs, N. (1955) The Middle Ordovician Of The Oslo Region, Norway. 6. Notes on bentonites (K-bentonites) from the Oslo-Asker district. Norsk Geologisk Tidsskrift 35, 29-52.

Hampton, B. D. (1989) Carbonate sedimentology of the Manzanita Member of the Cherry Canyon Formation, in Harris, P. M., and Grover, G. S., eds., Subsurface and outcrop examination of the Capitan shelf margin, Northern Delaware Basin: Society of Economic Paleontologists and Mineralogists Core Workshop 13, 431–439.

Haynes, J.T. (1994) The Ordovician Deicke and Millbrig K-bentonite beds of the Cincinnati Arch and the southern Valley and Ridge Province: Geological Society of America Special Paper, 290, 1-80.

Haynes, J.T., Melson, W.G., and Kunk, M.J. (1995) Composition of biotite phenocrysts in Ordovician tephras casts doubt on the proposed trans-Atlantic correlation of the Millbrig K-bentonite (United States) and the Kinnekulle K-bentonite (Sweden): Geology, 23, 847–850.

Histon, K., Klein, P., Schönlaub, H.P., and Huff, W.D. (2007) Lower Paleozoic K-bentonites from the Carnic Alps, Austria: Austrian Journal of Earth Sciences, 100, 26-42.

Holland, S.M., and Patzkowsky, M.E. (1996) Sequence stratigraphy and long-term paleoceanographic changes in the Middle and Upper Ordovician of the eastern United States. Geological Society of America Special Paper 306, 117–128.

Huff, W.D., and Türkmenoglu, A.G. (1981) Chemical characteristics and origin of Ordovician K-bentonites along the Cincinnati arch: Clays and Clay Minerals, 29, 113-123.

Huff, W.D., and Kolata, D.R. (1990) Correlation of the Ordovician Deicke and Millbrig K-bentonites between the Mississippi Valley and the southern Appalachians: American Association of Petroleum Geologists Bulletin, 74, 1736-1747.

Huff, W.D., Bergström, S.M., and Kolata, D.R. (1992) Gigantic Ordovician volcanic ash fall in North America and Europe: Biological, tectonomagmatic, and event-stratigraphic significance: Geology, 20, 875–878.

Huff, W.D., Merriman, R.J., Morgan, D.J., and Roberts, B. (1993) Distribution and tectonic setting of Ordovician K-bentonites in the United Kingdom: Geological Magazine, 130, 93–100.

Huff, W.D., and Bergström, S.M. (1995) Castlemainian K-bentonite beds in the Ningkuo Formation of the Jiangshan Province - The first Lower Ordovician K-bentonites found in China: Palaeoworld, 5, 101-105.

Huff, W.D., Kolata, D.R., Bergström, S.M., and Zhang, Y.-S. (1996a) Large-magnitude Middle Ordovician volcanic ash falls in North America and Europe: dimensions, emplacement and post-emplacement characteristics: Journal of Volcanology and Geothermal Research, 73, 285-301.

Huff, W.D., Morgan, D.J., and Rundle, C.C. (1996b) Silurian K-bentonites of the Welsh Borderlands: Geochemistry, mineralogy and K-Ar ages of illitization: Nottingham, British Geological Survey, Technical Report, WG/96/45, 25 p.

Huff, W.D., Bergström, S.M., Kolata, D.R., Cingolani, C., and Astini, R.A. (1998) Ordovician K-bentonites in the Argentine Precordillera: relations to Gondwana margin evolution, in Pankhurst, R.J., and Rapela, C.W., eds., The Proto-Andean Margin of Gondwana. Geological Society, London, Special Publications, 142, 107-126.

Huff, W.D., Mu□ftu□oglu, E., Kolata, D.R., and Bergström, S.M. (1999) K-bentonite bed preservation and its event stratigraphic significance: Acta Universitatis Carolinae — Geologica, 43, 491–493.

Huff, W.D., Bergström, S.M., and Kolata, D.R. (2000) Silurian K-bentonites of the Dnestr Basin, Podolia, Ukraine: Geological Society of London, Journal, 157, 493–504.

Huff, W.D., Mu□ftu□oglu, E., Bergström, S.M., and Kolata, D.R. (2004) Resolving questions of consanguinity between the late Ordovician Deicke, Millbrig and Kinnekulle K-bentonites in North America and Baltoscandia: Geological Society of America Abstracts with Programs, 36 (5), 246.

Huff, W.D. (2008) Ordovician K-bentonites: Issues in interpreting and correlating ancient tephras: Quaternary International, 178, 276-287.

Huff, W.D., Bergström, S.M., and Kolata, D.R. (2010) Ordovician explosive volcanism: In: Finney, S.C. and Berry, W. (Eds.) Earth system during the Ordovician Period: Geological Society of America Special Paper 466, 13-28.

Huff, W.D., Dronov, A.V., Sell, B., Kanygin, A.V., and Gonta, T.V. (2014) Traces of explosive volcanic eruptions in the Upper Ordovician of the Siberian Platform: Estonian Journal of Earth Sciences, 63 (4), 244-250.

Inanli, F.Ö., Huff, W.D., and Bergström, S.M. (2009) The Lower Silurian (Llandovery) Osmundsberg K-Bentonite In Baltoscandia and the British Isles: Chemical fingerprinting and regional correlation: GFF, 131, 269-279.

Jenkins, R.J.F., Cooper, J.A., and Compston, W. (2002) Age and biostratigraphy of Early Cambrian tuffs from SE Australia and southern China. Journal of the Geological Society, London, 159, 645–658.

Karaouia, B., Breitkreuzb, C., Mahmoudia, A., Youbic, N., Hofmanne, M., Gärtnere, A., and Linnemann, U. (2015) U–Pb zircon ages from volcanic and sedimentary rocks of the Ediacaran Bas Draâ inlier (Anti-Atlas Morocco): Chronostratigraphic and provenance implications. Precambrian Research, 263, 43-58.

Kay, G.M. (1935) Distribution of Ordovician altered volcanic materials and related clays: Geological Society of America Bulletin, 46, 225-244.

Kaljo, D., Hints, L., Martma, T., Nõlvak, J., and Oraspõld, A. (2004) Late Ordovician carbon isotope trend in Estonia, its significance in stratigraphy and environmental analysis: Palaeogeography, Palaeoclimatology, Palaeoecology, 210, 165–185.

Kiipli, T., Kallaste, T., Nestor, V., and Loydell, D.K. (2010) Integrated Telychian (Silurian) K-bentonite chemostratigraphy and biostratigraphy in Estonia and Latvia. Lethaia 43 (1) 32-44.

Kiipli, T., Kallaste, T., Nielsen, A.T., Schovsbo, N.H., and Siir, S. (2014a) Geochemical discrimination of the Upper Ordovician Kinnekulle Bentonite in the Billegrav-2 drill core section, Bornholm, Denmark. Estonian Journal of Earth Sciences, 63 (4) 264-270.

Kiipli, T., Radzevičius, S., and Kallaste, T. (2014b) Silurian bentonites in Lithuania: correlations based on sanidine phenocryst composition and graptolite biozonation - interpretation of volcanic source regions. Estonian Journal of Earth Sciences, 63 (1), 18-29.

King, P.B. (1948) Geology of the southern Guadalupe Mountains, Texas. U.S. Geological Survey Professional Paper 215, 183pp.

Knight, W.C. (1897) Mineral soap: Engineering and Mining Journal, 63, 600-601.

Knight, W.C. (1898) Bentonite: Engineering and Mining Journal, 66, 491.

Kolata, D.R., Frost, J.K., and Huff, W.D. (1987) Chemical correlation of K-bentonites in the Middle Ordovician Decorah Subgroup, upper Mississippi Valley: Geology, 15, 208-211.

Kolata, D.R., Huff, W.D., and Bergström, S.M. (1996) Ordovician K-bentonites of eastern North America: Geological Society of America Special Paper 313, 1-84.

Kolata, D.R., Huff, W.D., and Bergström, S.M. (1998) Nature and regional significance of unconformities associated with the Middle Ordovician Hagan K-bentonite complex in the North American midcontinent: Geological Society of America Bulletin, 110, 723-739.

Koren', T.N., Abushik, A.F., Modzalevskaya, T.L., and Predtechensky, N.N. (1989) Podolia. In: C. H. Holland and M. G. Bassett (eds) A Global Standard for The Silurian System. National Museum of Wales, Cardiff, 141-149.

Laufeld, S., and Jeppsson, L. (1976) Silicification and bentonites in the Silurian of Gotland. Geologiska Föreningens i Stockholrn Forhandlingar, 98, 313-344.

Leslie, S.A., Bergström, S.M., and Huff, W.D. (2006) Volcanic ash beds discovered in the Upper Bromide Formation and Womble Shale (Ordovician) in Oklahoma: The westernmost occurrences of the Millbrig and Deicke K-bentonites?: Geological Society of America Abstracts with Programs, 38, p. 67.

Lowe, D.J. (2011) Tephrochronology and its application: a review. Quaternary Geochronology, 6, 107-153.

Lyons, P.C., Spears, D.A., Outerbridge, W.F., Congdon, R.D., and Evans, H.T. Jr. (1994) Euramerican tonsteins: overview, magmatic origin, and depositional-tectonic implications. Palaeogeography, Palaeoclimatology, Palaeoecology, 106, 113-134.

Lyons, P.C., Krogh, T.E., Kwok, Y.Y., Davis, D.W., Outerbridge, W.F., and Evans Jr., H.T. (2006) Radiometric ages of the Fire Clay tonstein [Pennsylvanian (Upper Carboniferous), Westphalian, Duckmantian]: A comparison of U–Pb zircon single-crystal ages and ^{40}Ar/^{39}Ar sanidine single-crystal plateau ages, International Journal of Coal Geology 67, 259–266.

Martini, J.E.J. (1974) On the presence of ash beds in volcanic fragments in the graywacke of the Karoo System in Southern Cape Province (South Africa). Transactions of the Geological Society of South Africa, 77, 113-116.

Maynard, J.B., Chocyk-Jaminski, M., Gaines, R.R., Huff, W.D., Krekeler, M.P., Prokopenko, M., and Summers, A.M. (1996) Bentonites in the Late Permian (Tatarian) Irati Formation of Brazil; geochemistry and potential for stratigraphic correlation: Abstracts with Programs - Geological Society of America, 28 (7), 280.

McKerrow, W.S., Dewey, J.F., and Scotese, C.R. (1991) The Ordovician and Silurian development of the Iapetus Ocean: Special Papers in Palaeontology, 44, 165–178.

McLachlan, I.R., and Jonker, J.P. (1990) Tuff beds in the northwestern part of the Karoo Basin. South African Journal of Geology, 93, 329-338.

Meek, F.B., and Hayden, F.V. (1862) Description of new Lower Silurian (Primordial), Jurassic, Cretaceous and Tertiary fossils, collected in Nebraska Territory, with some remarks on the rocks from which they were obtained: Philadelphia Academy of Natural Sciences Proceedings, 13, 415-447.

Millward, D., and Stone, P. (2012) Stratigraphical framework for the Ordovician and Silurian sedimentary strata of northern England and the Isle of Man. British Geological Survey, Geology and Landscape, England, Research Report RR/12/04, 122 p.

Moore, D.M., and Reynolds, R.C. (1997) X-Ray Diffraction and the Identification and Analysis of Clay Minerals: New York, Oxford University Press, 378 p.

Nelson, W.A. (1921) Notes on a volcanic ash bed in the Ordovician of Middle Tennessee: Tennessee Division of Geology Bulletin 25, 46-48.

Nelson, W.A. (1922) Volcanic ash beds in the Ordovician of Tennessee, Kentucky and Alabama: Geological Society of America Bulletin, 33, 605-615.

Newell, N.D., Rigby, J.K., Fischer, A.G., Whiteman, A.J., Hickox, J.E., and Bradley, J.S. (1953) The Permian Reef Complex of Guadalupe Mountains Region, Texas and New Mexico. San Francisco: W.H. Freeman & Company, 236 p.

Nicklen, B.L., Bell, G.L. Jr., and Huff, W.D. (2007) Ancient ash beds in the type area of the Middle Permian, Guadalupe Mountains National Park, west Texas, USA: Geological Society of America Abstracts with Programs, 39 (6), 148.

Nicklen, B.L. (2011) Establishing a Tephrochronologic Framework for the Middle Permian (Guadalupian) Type Area and Adjacent Portions of the Delaware Basin and Northwestern Shelf, West Texas and Southeastern New Mexico, USA, unpublished PhD dissertation, University of Cincinnati, 134 p.

Nikiforova, O.I. (1977) Podolia. In: A. Martinsson (ed.) The Silurian-Devonian boundary. Schweizerbartsche Verlagsbuchhandlung, Stuttgart, 52-64.

Nordgulen, Ø., Barnes, C.G., Pedersen, R.B., Skår, Ø., and Yoshinobu, A.S. (2003) Mid Ordovician to Early Silurian granitoid plutonism in the Scandinavian Caledonides: Geological Society of America Abstracts with Programs, 35 (7), 346.

Pearce, J.A., Harris, N.B.W., and Tindle, A.G. (1984) Trace element discrimination diagrams for the tectonic interpretation of granitic rocks. Journal of Petrology, 25: 956-983.

Pellenard, P., Deconinck, J-F., Huff, W.D., Thierry, J., Marchand, D., Fortwengler, D., and Trouiller, A., (2003) Characterization and correlation of Upper Jurassic (Oxfordian) bentonite deposits in the Paris Basin and the Subalpine Basin, France, Sedimentology 50, 1035–1060.

Pellenard, P., Nomade, S., Martire, L., De Oliveira Ramalho, F., Monna, F., and Guillou, H. (2013) The first ^{40}Ar–^{39}Ar date from Oxfordian ammonite-calibrated volcanic layers (bentonites) as a tie-point for the Late Jurassic. Geological Magazine 150 (6), 1136-1142.

Poiré, D.G., Spalletti, L.A., and Del Valle, A. (2003) The Cambrian-Ordovician siliciclastic platform of the Balcarce Formation (Tandilia System, Argentina): Facies, trace fossils, palaeoenvironments and sequence stratigraphy: Geologica Acta, 1, 41–60.

Price, N.B., and Duff, P. McI. D. (1969) Mineralogy and chemistry of tonsteins From Carboniferous sequences in Great Britain, Sedimentology 13, 45-69.

Ross, C.S., and Shannon, E. V. (1926) The minerals of bentonite and related clays and their physical properties: Journal of the American Ceramic Society, 9, 77-96.

Ross, C.S. (1928) Altered Paleozoic Volcanic Materials and Their Recognition, Bulletin American Association of Petroleum Geologists, 12 (2), 143-164.

Ross, R.J., Jr., and Naeser, C.W. (1984) The Ordovician time scale—New refinements, in Bruton, D., ed., Aspects of the Ordovician System: Palaeontological contributions from the University of Oslo, 295, 5–10.

Rowley, D.B., and Kidd, W.S.F. (1981) Stratigraphic relationships and detrital composition of the medial Ordovician flysch of western New England: Implications for the tectonic evolution of the Taconic orogeny: Journal of Geology, 89, 199–218.

Rubidge, B.S., Erwin, D.H., Ramezani, J., Bowring, S.A., and de Klerk, W.J. (2013) High-precision temporal calibration of Late Permian vertebrate biostratigraphy: U-Pb zircon constraints from the Karoo Supergroup, South Africa. Geology, 41(3), 363-366.

Santos, R.V., Souza, P.A., de Alvarenga, C.J.S., Dantas, E.L., Pimentel, M.M., de Oliveira, C.G., and de Araújo, L.M. (2006) Shrimp U–Pb zircon dating and palynology of bentonitic layers from the Permian Irati Formation, Paraná Basin, Brazil, Gondwana Research, 9 (4), 456-463.

Saylor, B.Z., Poling, J.M., and Huff, W.D. (2005) Stratigraphic and chemical correlation of volcanic ash beds in the terminal Proterozoic Nama Group: Geological Magazine, 142, 519-538.

Schönlaub, H.P. (1992) Stratigraphy, biogeography and paleoclimatology of the Alpine Palaeozoic and its implications for plate movements: Jahrbuch Geologische Bundesanstalt, v. 135, p. 381–418.

Schönlaub, H.P. (1993) Stratigraphy, biogeography and climatic relationships of the Alpine Palaeozoic, in von Raumer, J.F., and Neubauer, F., eds., Pre-Mesozoic Geology in the Alps: New York, Springer-Verlag, 65–91.

Scotese, C.R., and McKerrow, W.S. (1991) Ordovician plate tectonic reconstructions, in Barnes, C.R., and Williams, S.H., eds., Advances in Ordovician Geology: Geological Survey of Canada Paper 90-9, 271–282.

Schoner, A.E. (1985) The Clinch Sandstone (Lower Silurian) along Highway 25E at Beans Gap. In K.R. Walker (ed.): The geologic history of the Thorn Hill Paleozoic section (Cambrian–Mississippian), eastern Tennessee: University of Tennessee, Department of Geological Sciences, Studies in Geology 10, 100–110.

Sell, B., Ainsaar, L., and Leslie, S. (2013) Precise timing of the Late Ordovician (Sandbian) supereruptions and associated environmental, biological, and climatological events. Journal of the Geological Society, London, Vol. 170, 2013, pp. 711–714.

Siddaiah, N.S., and Kumar, K. (2008) Tonsteins (altered volcanic ash) from Late Paleocene (~58.7-55.8 Ma) Sediments of the Northwest Sub-Himalaya and their Significance for the Timing of Initiation of India–Asia Collision, Memoir Geological Society Of India 72, pp. 145-164.

Simas, M.W., Guerra-Sommer, M., Mendonça Filho, J.G., Cazzulo-Klepzig, M., Formoso, M.L.L. and Degani-Schmidt, I. (2013) An accurate record of volcanic ash fall deposition as characterized by dispersed organic matter in a lower Permian tonstein layer (Faxinal Coalfield, Paraná Basin, Brazil). Geologica Acta, 11 (1), 45-57.

Sliaupa, S. (2000) Ordovician-Silurian metabentonites in the Baltic basin: A record of surrounding Caledonian volcanic activity: Geophysical Journal, 22, 128–129.

Smiley, T. (1985) The geology and climate of an indigenous forest, Petrified Forest National Park, Arizona. Bulletin of the Museum of Northern Arizona, 54, 9-15.

Spears, D.A., and Duff, P. Mcl. D. (1984) Kaolinite and mixed-layer illite-smectite in Lower Cretaceous bentonites from the Peace River coalfield, British Columbia. Canadian Journal of Earth Sciences 21, 465-476

Spears, D.A. (2012) The origin of tonsteins, an overview, and links with seatearths, fireclays and fragmental clay rocks. International Journal of Coal Geology 94, 22–31.

Środoń, J., Clauer, N., Huff, W., Dudek, T., and Banaś, M. (2009) K-Ar dating of the Lower Palaeozoic K-bentonites from the Baltic Basin and the Baltic Shield: implications for the role of temperature and time in the illitisation of smectite. Clay Minerals 44 (3), 361–387.

Środoń, J., Paszkowski, M., Drygant, D., Anczkiewicz, A., and Banaś, M. (2013) Thermal history of Lower Paleozoic rocks on the peri-Tornquist margin of the east European craton (Podolia, Ukraine) inferred from combined XRD, K-Ar, and AFT data. Clays and Clay Minerals 61 (2), 107–132.

Stanley, R.S., and Ratcliffe, N.M. (1985) Tectonic synthesis of the Taconian orogeny in western New England: Geological Society of America Bulletin, 96, 1227–1250.

Strauss, P.G. (1971) Kaolin-rich rocks in the East Midlands Coalfields of England. Proceedings 6th International Congress on Carboniferous Stratigraphy and Geology 4, 1519–1533.

Su, W.-B., He, L.-Q., Baum, G.R., Huff, W.D., and Li, Z.-M. (2004) K-bentonites near the Ordovician-Silurian boundary in South China: Contributing factors to the terminal Ordovician multiple-sphere crises?: Florence, Italy, International Geological Congress, 32nd, Abstracts Volume, 989.

Su, W.-B., Zhang, S., Huff, W.D., Li, H., Ettensohn, F.R., Chen, X., Yang, H., Han, Y., Song, B., and Santosh M. (2008) SHRIMP U–Pb ages of K-bentonite beds in the Xiamaling Formation: Implications for revised subdivision of the Meso- to Neoproterozoic history of the North China Craton: Gondwana Research, 14, 543–553.

Su, W.-B., Huff, W.D., Ettensohn, F.R., Liu, X., Zhang, J.E., and Li, Z. (2009) K-bentonite, black-shale and flysch successions at the Ordovician–Silurian transition, South China: possible sedimentary responses to the accretion of Cathaysia to the Yangtze Block and its implications for the evolution of Gondwana: Gondwana Research, 15, 111–130.

Sylvest, N.E, Borell, A.M., Brafford, J.A., Haneberg-Diggs, D., Huff, W.D., Huvaj, Y.N., Maynard, J. B., and Wasserstrom, L.W. (2012) Coeval Permian Bentonites in Brazil and South Africa, Geological Society of America Abstracts with Programs, 44 (7), 562.

Thomas, W.A., and Astini, R.A. (1996) The Argentine Precordillera: A traveler from the Ouachita embayment of North American Laurentia: Science, 273, 752–757.

Trewin, N.H., MacDonald, D.I.M., and Thomas, C.G.C. (2002) Stratigraphy and sedimentology of the Permian of the Falkland Islands: lithostratigraphic and palaeoenvironmental links with South Africa: Journal of the Geological Society, London, 159, 5-19.

Thompson, J.E., and Duff, P.G. (1965) Bentonite In The Upper Permian Black Alley Shale Bowen Basin Queensland. Bureau of Mineral Resources, Geology and Geophysics Report 171, 11p.

Thorarinsson, S. (1944) Tefrokronoliska studier på Island. (Tephrochronological studies in Iceland). Geografiska Annaler, 26, 1-217

Tomczyk, H. (1970) The Silurian, in Sokolowski, S., ed., The Geology of Poland, Volume 1:Warsaw, Wydawnictwa Geologiczne, 237–320.

Triplehorn, D.M., Turner, D.L., and Naeser, C.W. (1984) Radiometric age of the Chickaloon Formation of south central Alaska; Location of the Paleocene-Eocene boundary. Geological Society of America Bulletin 95, 640-742.

Triplehorn, D.M. (1990) Applications of tonsteins to coal geology: some examples from western United States, International Journal of Coal Geology, 16, 157-160

Tsegelnjuk, P.D. (1980a) The Rukshin and Tsyganka Series (the Upper Silurian-Lower Devonian) of Podolia and Volyn'. Institute of Geology, Academy of Sciences of the Ukrainian SSR, Kiev, 55.

Tsegelnjuk, P.D. (1980b) The Yaruga and Malinovtsy Series (the Lower-Upper Silurian) of Podolia and Volyn'. Institute of Geology, Academy of Sciences of the Ukrainian SSR, Kiev, 53.

Tucker, R.D., and Robinson, P. (1990) Age and setting of the Bronson Hill magmatic arc: A re-evaluation based on U-Pb zircon ages in southern New England: Geological Society of America Bulletin, 102, 1404–1419.

Ulrich, E.O. (1888) Correlation of the Lower Silurian horizons of Tennessee and of the Ohio and Mississippi valleys with those of New York and Canada: American Geologist, 1, 100 -110.

Uysal, I.T., Suzanne D. Golding, S.D., and Audsley, F. (2000) Clay-mineral authigenesis in the Late Permian coal measures, Bowen Basin, Queensland, Australia. Clays and Clay Minerals, 48 (3), 351-365.

Ver Straeten, C.A. (2004) K-bentonites, volcanic ash preservation, and implications for Early to Middle Devonian volcanism in the Acadian orogen, eastern North America: Geological Society of America Bulletin, 116, 474-489.

Weaver, B.L. (1991) Trace element evidence for the origin of ocean-island basalts. Geology, 19, 123-126.

Weaver, C.E. (1953) Mineralogy and petrology of some Ordovician K-bentonites and related limestones. Bulletin of the Geological Society of America 64, 921-944.

Weaver, C.E. (1989) Clays, Muds and Shales. Developments in Sedimentology 44: Elsevier, Amsterdam, 819 p.

Wilson, C.W., Jr. (1949) Pre-Chattanooga stratigraphy in central Tennessee, Tennessee Division of Geology, Bulletin, 56, 407 p.

Wilson, R.F., and Stewart, J.H. (1967) Correlation of Upper Triassic and Triassic (?) formations between southwestern Utah and southern Nevada. United States Geological Survey Bulletin 1244-D, 20 p.

Wilson, M., and Guiraud, R. (1998) Late Permian to Recent magmatic activity on the African-Arabian margin of Tethys. In: MacGregor, D. S., Moody, R. T. J. and Clark-Lowes, D. D. (eds) Petroleum Geology of North Africa. Geological Society of London, Special Publication 132, 231-263.

Winchester, J.A., and Floyd, P.A. (1977) Geochemical discrimination of different magma series and their differentiation products using immobile elements: Chemical Geology, 20, 325–343.

Zhang, J., Li, G., and Zhou, C. (1997) Geochemistry of light colour clayrock layers from the Early Cambrian Meishucun Stage in eastern Yunnan and their geological significance [in Chinese]: Acta Petrologica Sinica, 13, 100–110.

Zhou, Y., Bohor, B.F., and Ren, Y. (2000) Trace element geochemistry of altered volcanic ash layers (tonsteins) in Late Permian coal-bearing formations of eastern Yunnan and western Guizhou Province, China. International Journal of Coal Geology 44, 305–324.

Zhou, M., Luo, T., Liu, S., Qian, Z., and Xing, L. (2013) SHRIMP zircon age for a K-bentonite in the top of the Laobao Formation at the Pingyin section, Guizhou, South China. Science China: Earth Sciences, 56 (10), 1677-1687.

Zhou, M., Luo, T., Huff, W.D., and Liu, S. (2014) Prominent Lower Cambrian K-Bentonites In South China: Distribution, Mineralogy, and Geochemistry: Journal of Sedimentary Research, 84, 842-853.

****

Figure 1: Stratigraphic columns of the Kuibis and Schwarzrand subgroups (a) in the vicinity of Witputs in the Witputs subbasin and (b) along the Zebra River in the Zaris subbasin showing positions of dated and undated ash beds, fossil distributions and stratigraphic variation in $\delta^{13}C$ of carbonate units (after Saylor et al. 2005).

Figure 2: Representative sections from the Precambrian-Cambrian transitional strata of the Yangtze Block showing the stratigraphic position and regional correlation of two key K-bentonite beds (after Zhou et al. 2014).

Figure 3: Stratigraphic columns of the Precambrian-Cambrian sequences in the Kunming (A) and Zunyi (B) regions. DYF, DH, ZYC, DB, and BYS denote the Dengying Formation, and the Dahai, Zhongyicun, Daibu, and Baiyanshao Members, respectively (after Zhou et al. 2008).

Figure 4: Stratigraphic distribution of the Deicke and Millbrig K-bentonites in the southern Appalachian basin. Note: Pencil Cave and Mud Cave are drillers' names previously applied to the Deicke and Millbrig K-bentonites, respectively (after Huff 2008).

Figure 5: (a) Core showing a K-bentonite (arrow) in a carbonate section, (b) Roadcut at Gladeville, TN, with Deicke (D) and Millbrig (M) separated by about 4m of Eggleston Fm. limestone, (c) Deicke 3.2m below the Millbrig in the Decorah Fm. at Minke Hollow, MO, and (d) Deicke in the Eggleston Fm. at Carthage, TN (after Huff 2008).

Figure 6: Transatlantic correlation diagram, showing the relations between conodont, graptolite and chitinozoan biostratigraphy, K-bentonite event stratigraphy, and the early Chatfieldian $\delta^{13}C$ excursion in North America and Baltoscandia. On the basis of these relations, the GICE is considered the same $\delta^{13}C$ excursion as the "middle Caradocian" excursion of Kaljo et al. (2004) (after Bergström et al. 2010).

Figure 7: A tectonic discrimination diagram showing the position of the Cerro Viejo volcanic rocks in terms of granitic origins. WPG, within plate granite; ORG, ocean ridge granite; VAG, volcanic arc granite; syn-COLG, syn-collision granite. The samples fall on the boundary between volcanic arc and within plate granites, typical of collision margin felsic volcanic rocks (after Huff et al. 1998).

Figure 8: Quartz-hosted glass melt inclusions from Cerro Viejo were analyzed by electron microprobe and the data plotted in anhydrous form on a total alkali-silica (TAS) diagram. The high silica content indicates the glass is rhyolitic in composition. Field names are (I) andesite, (2) basaltic andesite, (3) picrobasalt, (4) tephrite, basanite, (5) trachybasalt, (6)

basaltic trachyandesite, (7) trachyandesite, (8) trachydacite, (9) phonotephrite, and (10) tephriphonolite (after Huff et al. 1998).

Figure 9: Global stratigraphic distribution of Ordovician K-bentonites (after Huff et al. 2010).

Figure 10: Stratigraphic distribution of K-bentonites recognized in the Carnic Alps (after Histon et al. 2007).

Figure 11: Correlation between typical Ordovician–Silurian transition K-bentonite-bearing sections in south China (after Su et al. 2009).

Figure 12: Stratigraphic distribution of Silurian K-bentonites in the Welsh Borderland (after Huff et al. 1996b).

Figure 13: Diagram showing proposed correlation of the Osmundsberg K-bentonite in a 1300 km long transect across Baltoscandia from north-central Sweden to western Estonia. Numbers to the right of each column indicate ash bed thickness in centimeters (after Bergström et al. 1998b).

Figure 14: Aeronian–Telychian K-bentonite bed succession along Linn Branch, Dob's Linn, 16 km northeast of Moffat, southern Scotland. Dotted ornament marks greywackes. Note the very large number (49) of individual ash beds (after Bergström et al. 1998b).

Figure 15: A composite stratigraphic column for the Silurian of the Dnestr Valley, Ukraine. K-bentonite beds are listed on the right with measured thickness (cm) given in parentheses. The stratigraphic positions of individual sections that were studied are included (after Huff et al. 2000).

Figure 16: Stratigraphic classification of the Silurian portion of the Arisaig Group showing the biostratigraphic position of intervals with K-bentonite beds (after Bergström et al 1997a).

Figure 17: Tectonic discrimination diagram plot of 12 Arisaig K-bentonites after the method of Pearce et al. (1984). WPG, within plate granite; ORG, ocean ridge granite; VAG, volcanic arc granite; syn-COLG, syn-collision granite. The trend from left to right generally follows decreasing stratigraphic age. The majority of beds plot in the field of within-plate granites and most likely represent an evolutionary development towards more felsic magmas during closure of the Iapetus Ocean.

Figure 18: The Acadian orogen, the Appalachian Foreland Basin, and the stratigraphy of Lochkovian to lower Givetian strata (Lower to Lower Middle Devonian), Appalachian Basin. A: Cross-sectional cartoon of the Appalachian foreland basin, the Acadian orogen, and the Avalon terrane. B: Eastern New York stratigraphic section of the study interval, showing position of major K-bentonite clusters and additional discrete beds. Nomenclature of correlative strata varies across the basin. Tioga A–G—Tioga A–G K-bentonite cluster; Tioga MCZ—Tioga middle coarse zone (after Ver Straeten 2004).

Figure 19: Carboniferous tonstein stratigraphy of Western Europe and North America (after Lyons et al. 1994).

Figure 20: Measured sections showing bentonite sample positions and interpreted correlations. Also shown is the position of the 265.3 ±0.2 Ma date of Bowring and others (1998b). The sections represent relative resistance of each interval and not the present erosional profile. The B-2 group is present in each section and is used as a datum. The Patterson Hills road cut section combines primary observations of the Manzanita interval with data from Diemer and others (2006) on the Lower Seven (after Nicklen 2011).

Figure 21: Outcrop and road cut sample localities of Permian K-bentonites (after Nicklen 2011).

Figure 22: Mg-Mn-Cl and Mg-Mn-Ce/Y diagrams of the apatite data from five K-bentonites at the Patterson Hills road cut, Guadalupe Mountains National Park (after Nicklen 2011).

Figure 23: K-bentonite layers in the Permian Collingham Formation, South Africa (after Sylvest et al. 2012).

Figure 24: Lithostratigraphy of the Falkland Islands Permian succession showing points of correlation with the equivalent South African succession (after Trewin et al. 2002).

Fig. 1

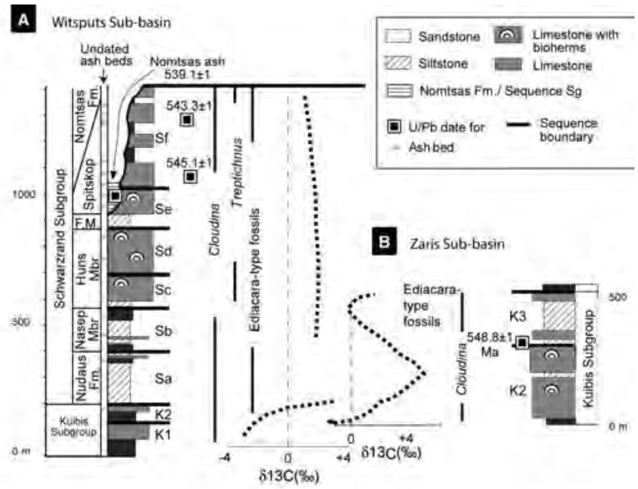
A
Witsputs Sub-basin
Undated ash beds
Nomtsas ash 539.1±1
543.3±1
545.1±1
Nomtsas Fm
Spitskop
F.M.
Huns Mbr
Nasep Mbr
Nudaus Fm
Schwarzrand Subgroup
Kuibis Subgroup
Sf
Se
Sd
Sc
Sb
Sa
K2
K1
Cloudina
Treptichnus
Ediacara-type fossils
1000
500
0 m
-4
0
+4
δ13C(‰)
Sandstone
Siltstone
Limestone with bioherms
Limestone
Nomtsas Fm./ Sequence Sg
U/Pb date for Ash bed
Sequence boundary
B
Zaris Sub-basin
Ediacara-type fossils
Cloudina
548.8±1 Ma
K3
K2
Kuibis Subgroup
500
0 m

Fig. 2

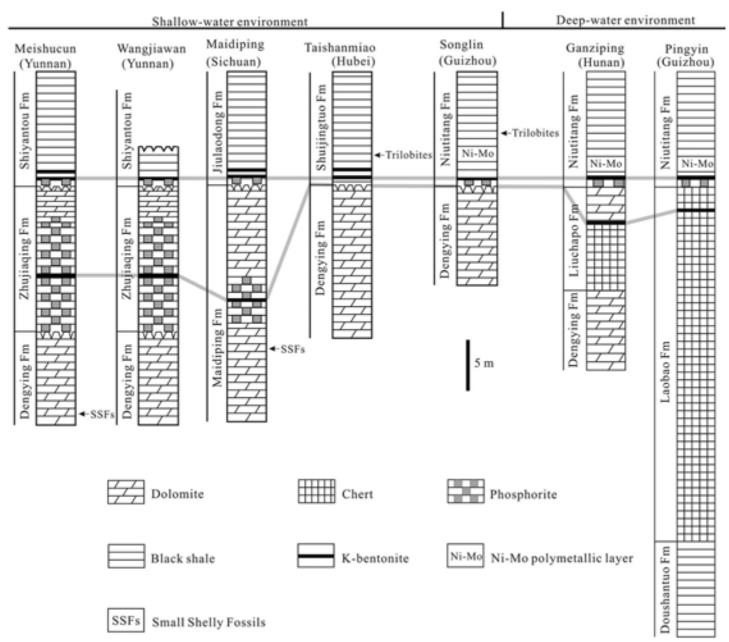
Shallow-water environment
Deep-water environment
Meishucun (Yunnan)
Wangjiawan (Yunnan)
Maidiping (Sichuan)
Taishanmiao (Hubei)
Songlin (Guizhou)
Ganziping (Hunan)
Pingyin (Guizhou)
Shiyantou Fm
Zhujiaqing Fm
Dengying Fm
Jiulaodong Fm
Maidiping Fm
Shuijingtuo Fm
Niutitang Fm
Liuchapo Fm
Laobao Fm
Doushantuo Fm
Trilobites
Ni-Mo
SSFs
5 m
Dolomite
Chert
Phosphorite
Black shale
K-bentonite
Ni-Mo polymetallic layer
Small Shelly Fossils

Fig. 3

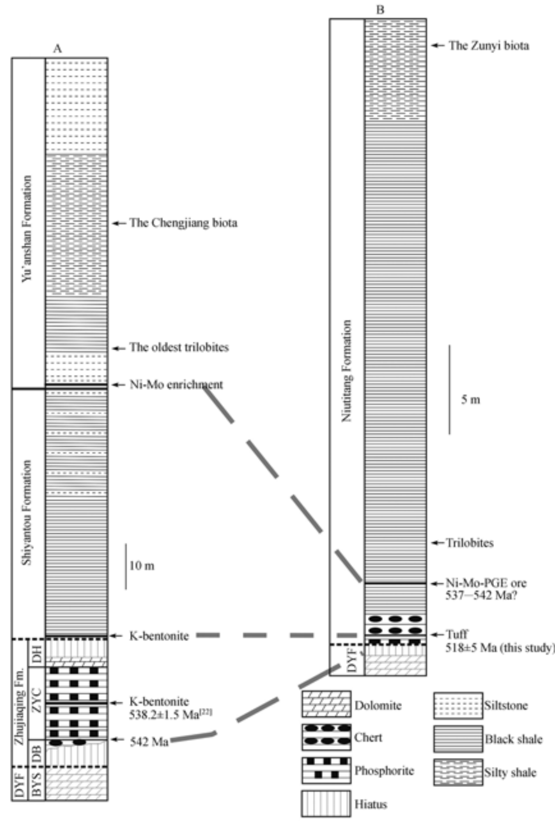
A
B
Yu'anshan Formation
Shiyantou Formation
Zhujiaqing Fm.
DH
ZYC
DB
DYF
BYS
The Chengjiang biota
The oldest trilobites
Ni-Mo enrichment
10 m
K-bentonite
K-bentonite
538.2±1.5 Ma[22]
542 Ma
The Zunyi biota
Niutitang Formation
5 m
Trilobites
Ni-Mo-PGE ore
537−542 Ma?
Tuff
518±5 Ma (this study)
DYF
Dolomite
Chert
Phosphorite
Hiatus
Siltstone
Black shale
Silty shale

Fig. 4

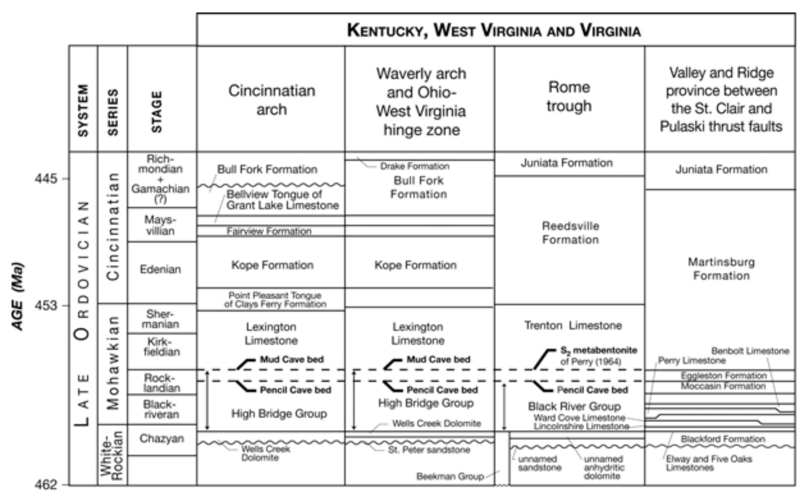
KENTUCKY, WEST VIRGINIA AND VIRGINIA
SYSTEM
SERIES
STAGE
Cincinnatian arch
Waverly arch and Ohio-West Virginia hinge zone
Rome trough
Valley and Ridge province between the St. Clair and Pulaski thrust faults
AGE (Ma)
445
453
462
LATE ORDOVICIAN
Cincinnatian
Mohawkian
White-Rockian
Rich-mondian + Gamachian (?)
Mays-villian
Edenian
Sher-manian
Kirk-fieldian
Rock-landian
Black-riveran
Chazyan
Bull Fork Formation
Bellview Tongue of Grant Lake Limestone
Fairview Formation
Kope Formation
Point Pleasant Tongue of Clays Ferry Formation
Lexington Limestone
Mud Cave bed
Pencil Cave bed
High Bridge Group
Wells Creek Dolomite
Drake Formation
Bull Fork Formation
Kope Formation
Lexington Limestone
Mud Cave bed
Pencil Cave bed
High Bridge Group
Wells Creek Dolomite
St. Peter sandstone
Beekman Group
Juniata Formation
Reedsville Formation
Trenton Limestone
S2 metabentonite of Perry (1964)
Pencil Cave bed
Black River Group
Ward Cove Limestone
Lincolnshire Limestone
unnamed sandstone
unnamed anhydritic dolomite
Juniata Formation
Martinsburg Formation
Benbolt Limestone
Perry Limestone
Eggleston Formation
Moccasin Formation
Blackford Formation
Elway and Five Oaks Limestones

Fig. 5

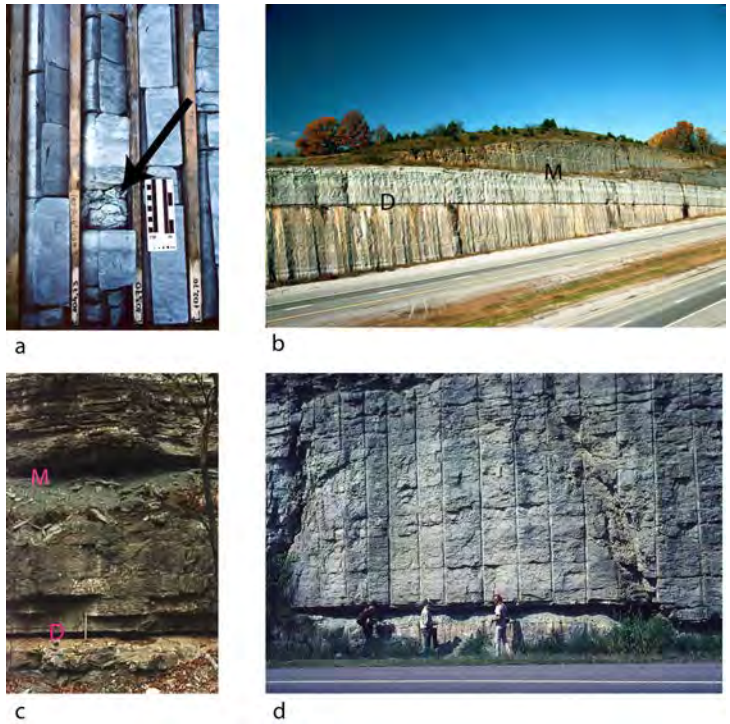
M
D
a
b
c
d

Fig. 6

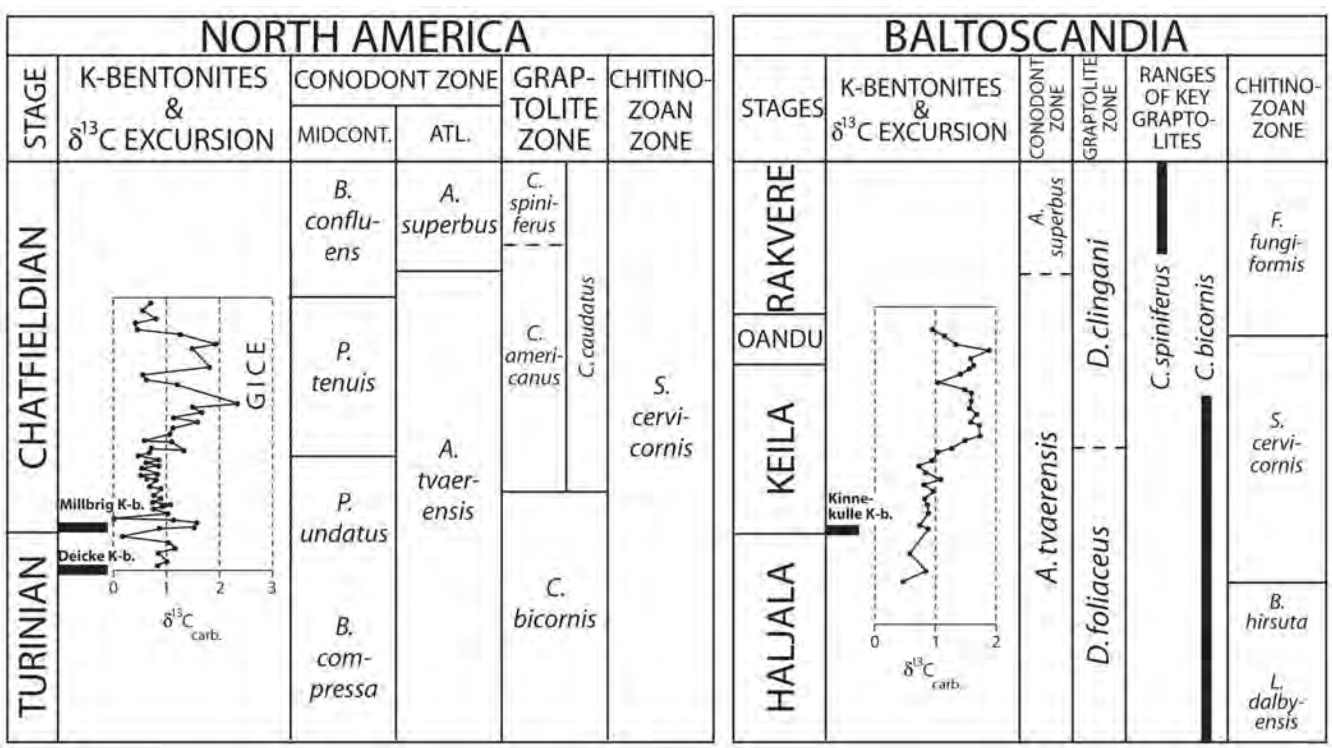
NORTH AMERICA
STAGE
K-BENTONITES & δ13C EXCURSION
CONODONT ZONE
MIDCONT.
ATL.
GRAPTOLITE ZONE
CHITINOZOAN ZONE
CHATFIELDIAN
TURINIAN
GICE
Millbrig K-b.
Deicke K-b.
0 1 2 3
δ13C carb.
B. confluens
P. tenuis
P. undatus
B. compressa
A. superbus
A. tvaerensis
C. spiniferus
C. americanus
C. caudatus
C. bicornis
S. cervicornis
BALTOSCANDIA
STAGES
K-BENTONITES & δ13C EXCURSION
CONODONT ZONE
GRAPTOLITE ZONE
RANGES OF KEY GRAPTOLITES
CHITINOZOAN ZONE
RAKVERE
OANDU
KEILA
HALJALA
Kinnekulle K-b.
0 1 2
δ13C carb.
A. superbus
A. tvaerensis
D. clingani
D. foliaceus
C. spiniferus
C. bicornis
F. fungiformis
S. cervicornis
B. hirsuta
L. dalbyensis

This is a preprint, the final version is subject to change, of the American Mineralogist (MSA)
Cite as Authors (Year) Title. American Mineralogist, in press.
(DOI will not work until issue is live.) DOI: http://dx.doi.org/10.2138/am-2016-5339CCBYNCND

Fig. 7

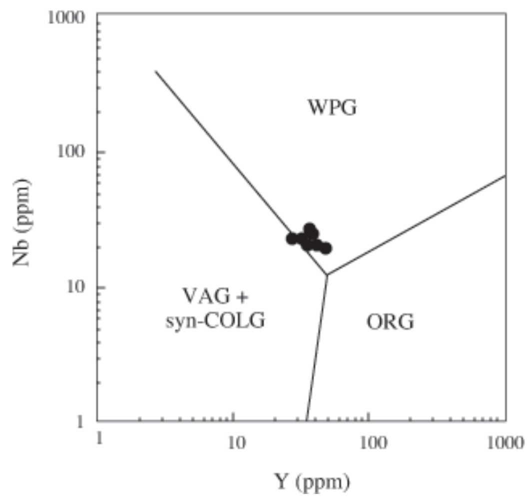

Fig. 8

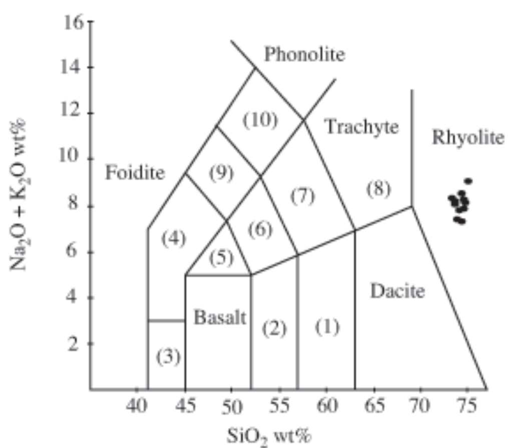

Fig. 9

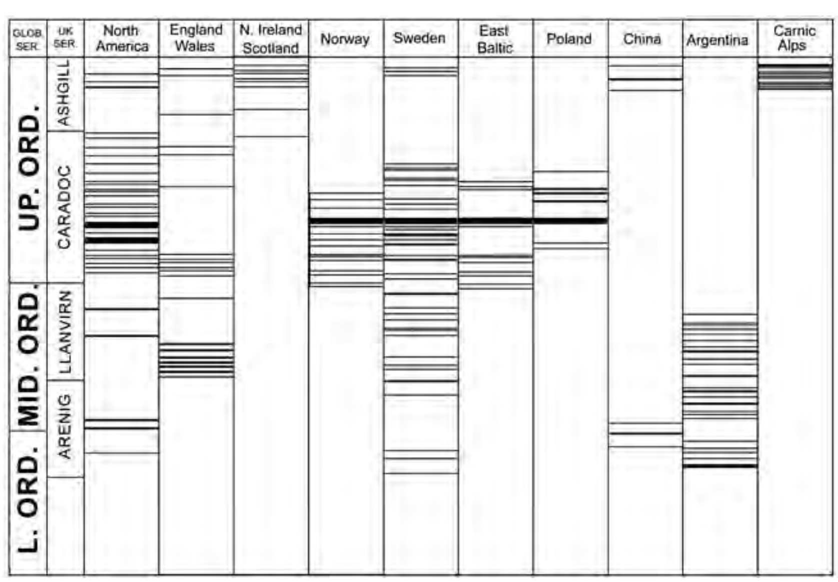

Fig. 10

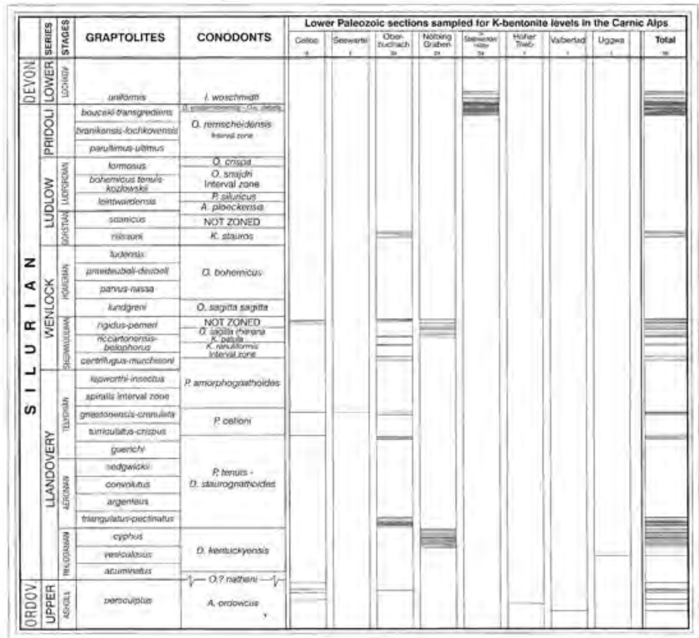

Fig. 11

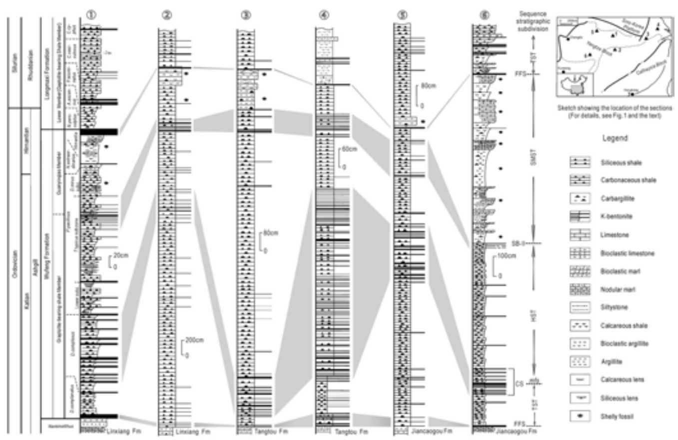

Fig. 12

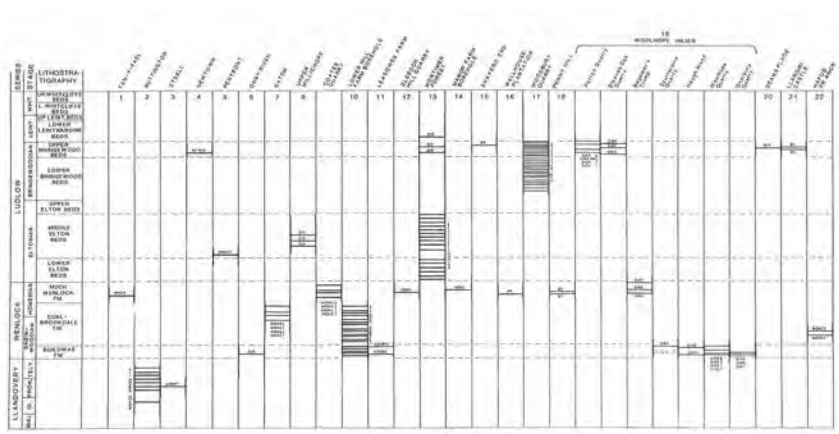

Fig. 13

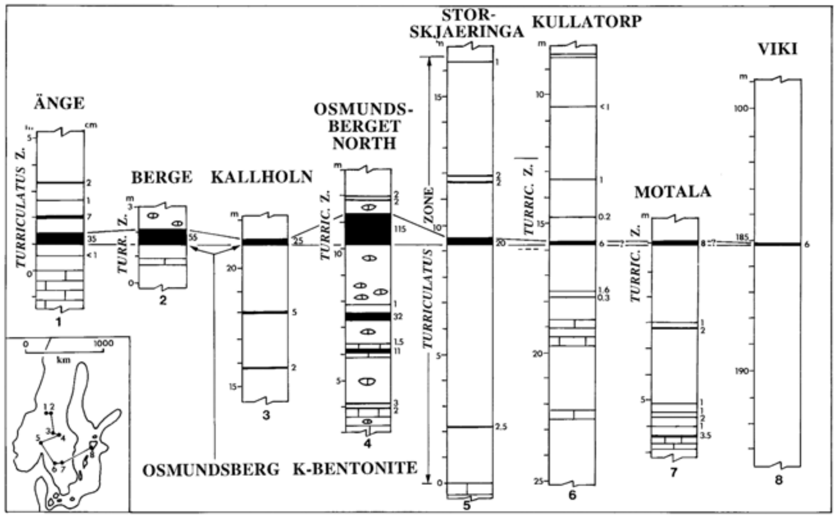
ÄNGE
BERGE
KALLHOLN
OSMUNDS-
BERGET
NORTH
STOR-
SKJAERINGA
KULLATORP
MOTALA
VIKI
TURRICULATUS Z.
TURR. Z.
TURRIC. Z.
TURRICULATUS
ZONE
TURRIC. Z.
TURRIC. Z.
OSMUNDSBERG K-BENTONITE
km

Fig. 14

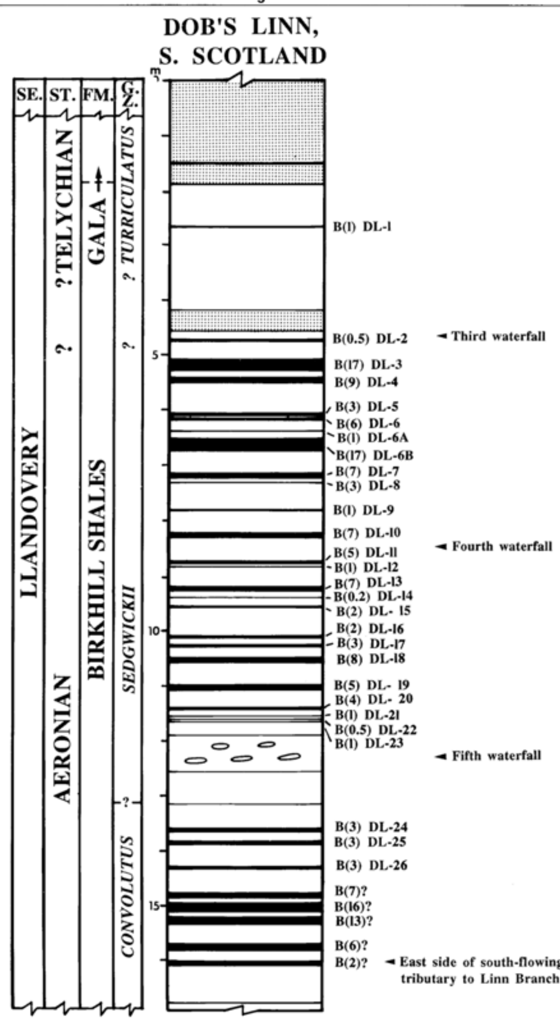
DOB'S LINN,
S. SCOTLAND
SE.
ST.
FM.
G. Z.
LLANDOVERY
?TELYCHIAN
AERONIAN
GALA
BIRKHILL SHALES
? TURRICULATUS
SEDGWICKII
CONVOLUTUS
B(l) DL-1
B(0.5) DL-2
Third waterfall
B(17) DL-3
B(9) DL-4
B(3) DL-5
B(6) DL-6
B(l) DL-6A
B(17) DL-6B
B(7) DL-7
B(3) DL-8
B(l) DL-9
B(7) DL-10
Fourth waterfall
B(5) DL-11
B(l) DL-12
B(7) DL-13
B(0.2) DL-14
B(2) DL-15
B(2) DL-16
B(3) DL-17
B(8) DL-18
B(5) DL-19
B(4) DL-20
B(l) DL-21
B(0.5) DL-22
B(l) DL-23
Fifth waterfall
B(3) DL-24
B(3) DL-25
B(3) DL-26
B(7)?
B(16)?
B(13)?
B(6)?
B(2)?
East side of south-flowing tributary to Linn Branch

Fig. 15.

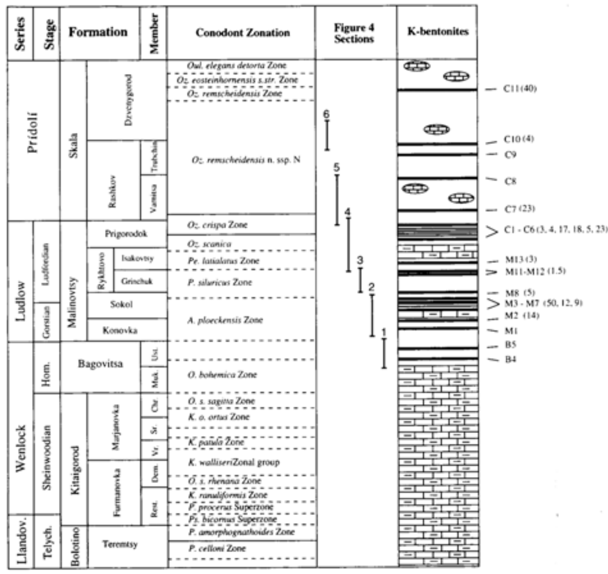

Fig. 16

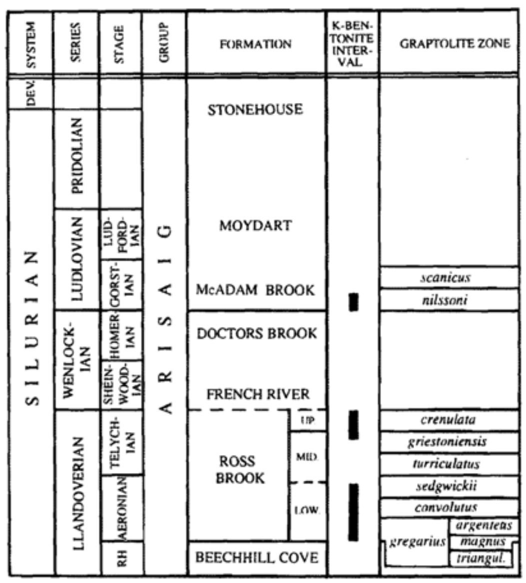

Fig. 17

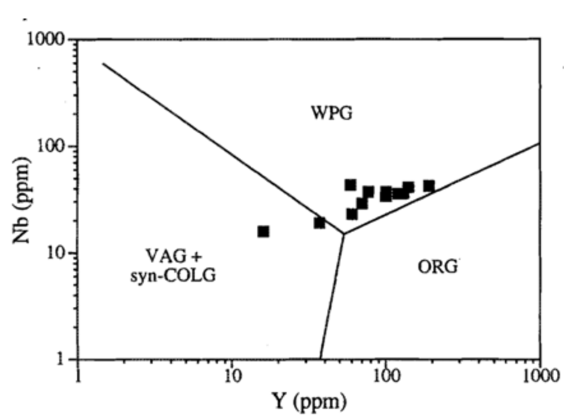

This is a preprint, the final version is subject to change, of the American Mineralogist (MSA)
Cite as Authors (Year) Title. American Mineralogist, in press.
(DOI will not work until issue is live.) DOI: http://dx.doi.org/10.2138/am-2016-5339CCBYNCND

Fig. 18

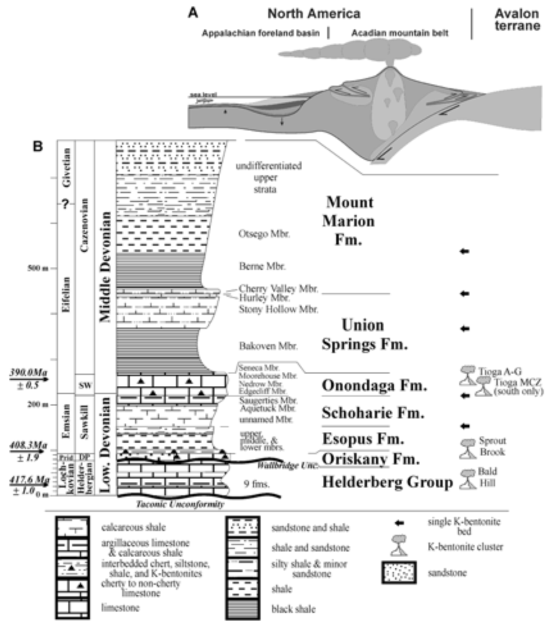

Fig. 19

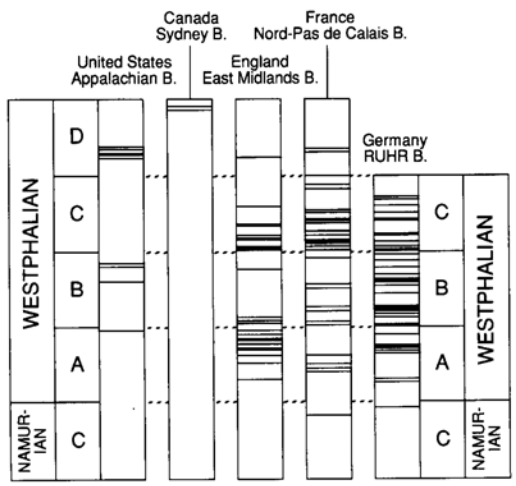

Fig. 20

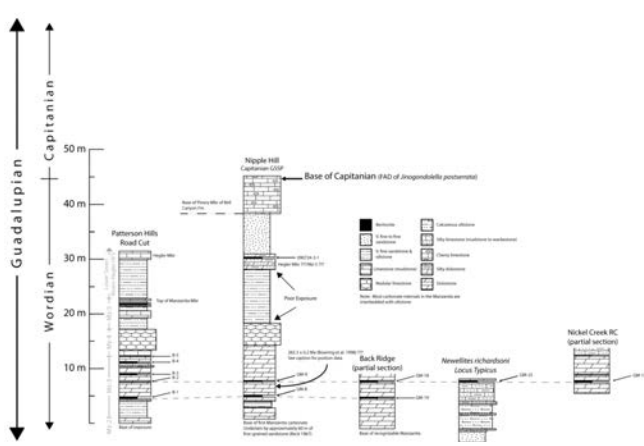

Fig. 21

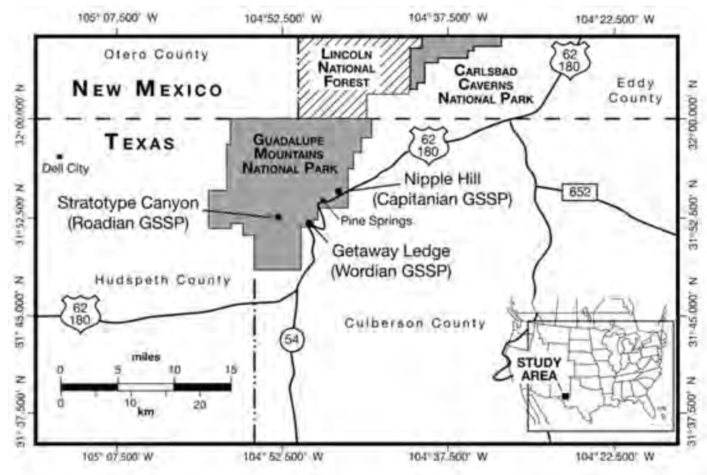

Fig. 22

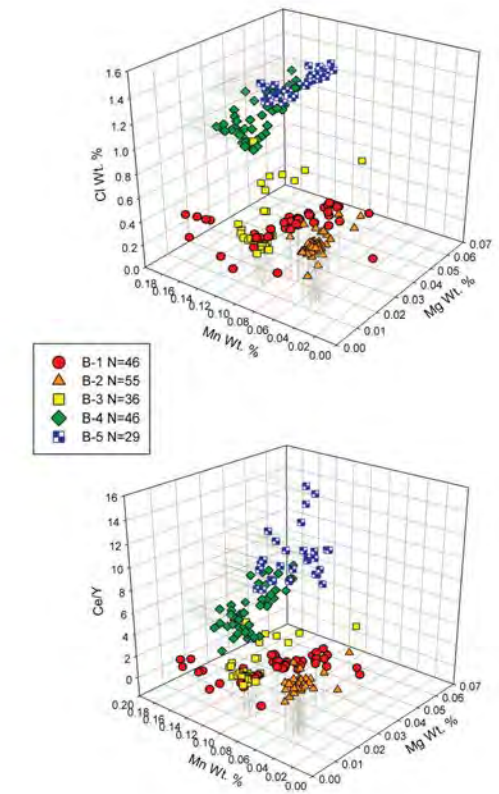

Fig. 23

Fig. 24